Resistance and Propulsion Characteristics of the VWS Hard Chine Catamaran Hull Series '89

Burkhard Müller-Graf (V)[1], **Dejan Radojčić** (M)[2], **Aleksandar Simić** (V)[2]

[1]VWS Berlin
[2]University of Belgrade

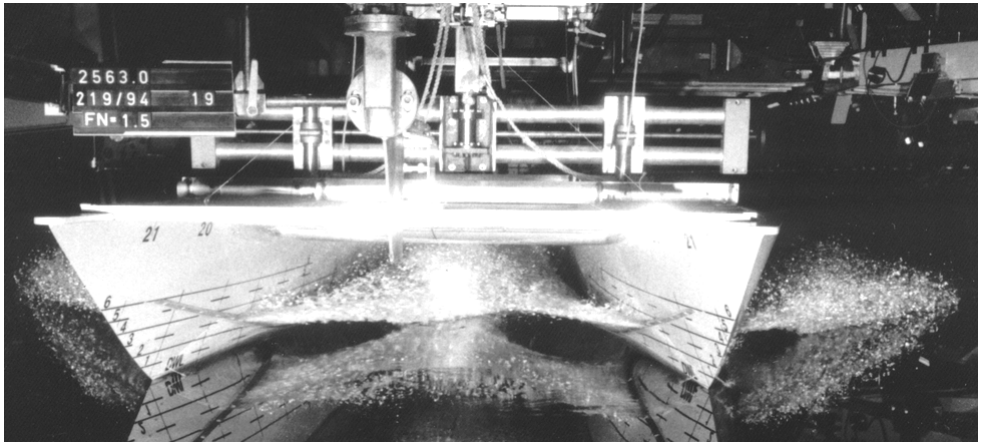

Hard chine catamaran with length-to-beam ratio of the demihulls of 11.55 at V=51 kt

In 1989 the Berlin Model Basin (VWS) started an R&D program for the development of a systematic series of hard chine catamarans. The series was intended to investigate the hydrodynamics of high-speed passenger and cargo catamarans of 20 to 60+ m length operating at speeds of 35 to 45 kt. Four length-to-beam ratios of the demihulls were tested (L_{WL}/B_{WLDH} = 7.55, 9.55, 11.55 and 13.55), with three midship deadrises (β_M = 38°, 27° and 16°) and different hull forms (symmetric, semi-symmetric and asymmetric hard chine forms and round bilge designs), afterbodies and propulsion configurations (fully wetted controllable and fixed-pitched propellers, surface piercing propellers and water-jets). An enormous quantity of data was gathered during 443 resistance tests and 132 self-propulsion tests carried out with relatively large models of between 3.6 and 5.1 m length, at speeds of up to 11 m/s. Tests were performed over a wide speed range, ranging from hump to planing speeds. Due to space limitations, only grouped results of the (so called) standard configuration (consisting of 12 models) are presented, although some non-standard configurations are also discussed. An immense stock of data are represented by the mathematical models – obtained through regression analysis – for resistance, trim, hull-propulsor interaction coefficients and delivered power. The tests and results were validated for trial conditions and thus are believed to be reliable.

For completeness the development of the VWS planing catamaran Series '89 is described in the first half of the paper, which is derived from several papers written by the first author. The regression models for predicting resistance and powering make up the core of this paper and are given in the second half. The paper covers its subject from a practical rather than theoretical viewpoint and will be of value to those who make performance predictions. The regression models are suitable for implementation in software and can replace "manual" powering predictions for the Series '89 planing catamarans.

NOMENCLATURE

Ae/Ao	-	Blade-area ratio
A_{FZ}	m^2	Area of zink anodes
A_V	m^2	Above-water transverse area projection
A_X	m^2	Area of two hull openings
B_T	m	Hull spacing at WL
B_{XDH}	m	Maximum breadth of demihull
C_{AA}	-	Air allowance coefficient
CBM	-	Block coefficient
C_{DP}	-	Structural rough. allowance coeff.
CM	-	Midship coefficient
Fn (Fn_L)	-	Froude number based on length
$Fn_{\nabla/2}$	-	Volumetric Froude number of the demihulls
g	m/s^2	Acceleration of gravity (9.81)
K_T	-	Thrust coefficient
K_Q	-	Torque coefficient
L_{WL}	m	Length of waterline
P_B	kW	Brake power
P_D	kW	Delivered power
P/D	-	Propeller pitch-diameter ratio
S (SWVO)	m^2	Wetted surface of the hull at rest without transom area
T_H	m	Draugh without keel
t_X	-	Thrust deduction fraction
V_S	m/s	Ship speed
V_W	m/s	Wind speed
WSC	-	Wetted surface coeff. ($S/(\nabla/2)^{2/3}$)
w_T	-	Wake fraction
z	-	Number of propeller blades
Δ (DISWAP)	t	Displacement mass
ΔC_F	-	Roughness allowance (0.0003)
∇ (DISV)	m^3	Displacement volume
β_M	deg	Angle of deadrise amidship
δ_W	deg	Angle of transom wedge
ε_B	-	Specific brake power ($P_B/\Delta g V_S$)
ε_R	-	Residuary drag-weight ratio ($R_R/\Delta g$)
ε_S	-	Specific total resistance ($R_{TS}/\Delta g$)
η_D	-	Quasi propulsive efficiency (P_E/P_D)
η_H	-	Hull efficiency
η_M	-	Gear and shaft losses
η_O	-	Propeller open-water efficiency
η_R	-	Relative rotative efficiency
θ	deg	Running trim angle
ν	m^2/s	Kinematic viscosity
ρ_A	kg/m^3	Mass density of air (1.226)
ρ_S	kg/m^3	Mass density of water

Subscripts

CAT	Catamaran
DH	Demihull
DW	Deadwood
MH	Monohull
S	Ship
TR	Trial condition
x	Horizontal
ψ	Axial (inclined)

INTRODUCTION

Catamarans can fulfill most of the requirements for high-speed passenger transportation, i.e. low power, large deck area, box shaped superstructures, good transverse stability, good course keeping and maneuverability. Consequently, in the 1980's a great need arose for this type vessel. However, only a few references concerning high-speed catamarans had been published (cf. Michel 1961, Clement 1962, Turner and Taplin 1968, Moss 1969, Thomas 1970, Fry and Graul 1972, Yermontayev, et al. 1977). These references did not give all information necessary for hull design, resistance and propulsion predictions, and seakeeping predictions. Confronted with a demand from shipyards for reliable powering predictions for high-speed catamarans, in 1988 the Berlin Model Basin (VWS) together with the German shipbuilding industry planned a comprehensive R&D program for high-speed catamarans. At about the same time systematic experiments were initiated in other institutions too, for instance at the University of Southampton (Insel and Moland 1992, Moland, et al. 1996, Moland and Lee 1997, Moland, et al. 2001) and MARINTEK (Werenskiold 1990).

This paper provides an overview of the VWS planing catamaran Series '89 and the results of the tests on the series. The details of the VWS Series '89 are documented in a number of papers and reports by the first author (Müller-Graf 1989, 1993a,b,c, 1994, 1996, 1999a,b, 2000). In addition Müller-Graf (1991) describes the novel spray rail system used on the designs, and Müller-Graf (1997) provides an in depth description of the resistance components, and trial and tank conditions. The other two authors are responsible for the numerical modeling of the enormous quantity of experimental data that were originally available only in the graphical form. As a tool, regression analysis was used throughout the numerical analysis – a few related papers treating the hydrodynamics of high-speed craft are Radojcic (1991), Radojcic and Matic (1997), and Radojcic, et al. (1997, 1999, 2001). Zips (1995) presents a regression analysis for evaluation of the Series '89 residuary resistance; this mathematical model is simpler and also less accurate than the models presented in this paper.

Preliminary Series and Results

To limit the number of form variants, the VWS R&D program started with a small preliminary series to answer the first questions one confronts when designing a high speed catamaran – which section shape and section symmetry properties should be chosen for the semi-planing and planing speed ranges.

In 1988 most passenger catamarans were 30–40 m long and had service speeds of 30–38 kt (corresponding to length Froude numbers Fn = 0.7–1.2). Hard chine section shapes were selected for the preliminary series since for speeds above Fn = 0.8 this section shape is optimal for resistance – it facilitates flow and spray separation (reducing frictional resistance) and the development of hydrodynamic lift (reducing pressure and frictional resistance through the emergence of the hull).

Three hard chine catamaran variants were designed and tested (see Figure 1):

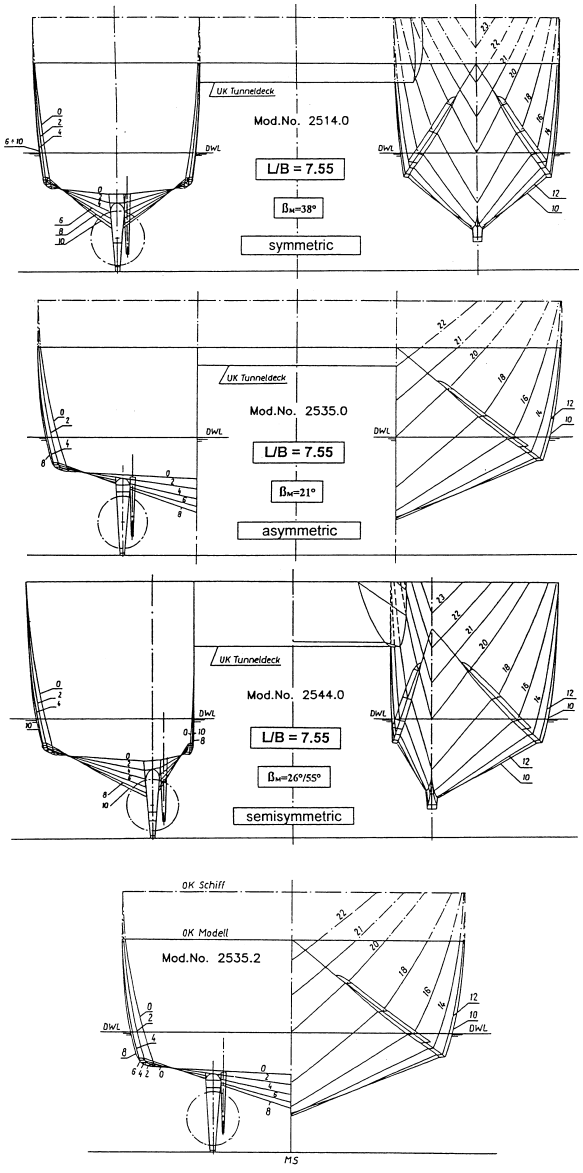

Figure 1 – Section plan of considered hulls during series development stage

- A form having symmetrical sections with the centerplane at $B_{XDH}/2$,
- A form with asymmetrical sections having the centerplane at the tunnel side of the demihull, and
- A semi-symmetrical form having the centerplane at $B_{XDH}/4$ on the inner or tunnel side of the demihull.

For the purpose of comparison, a fourth variant – a monohull – that was composed of two asymmetrical demihulls with no lateral separation was included in the series.

All four variants had model lengths of 3.9 m and were tested in calm water at two displacements, 4 to 6 different transom wedge inclinations, and speeds corresponding to Fn = 0.25–1.35.

To determine the interference drag for a tunnel width of B_T/L_{WL} = 0.167 (which was found to be the mean value of 96 actual catamarans having waterline lengths of 20 to 40 m) the resistance of a single demihull of each section type was tested at the half displacement of the catamaran configuration and at the same inclinations of the transom wedge. Propulsion tests were also performed for the design displacement and for the optimum wedge inclination, with fixed-pitch and controllable-pitch propellers of various diameters and pitch ratios. Consequently, on the basis of the results of 56 resistance tests, 12 propulsion tests and 3 seakeeping tests, the effect of section symmetry on resistance, propulsion and seakeeping characteristics were determined. The results were presented in 80 diagrams and are briefly discussed below.

a) The resistance tests indicated the following trends:

- Relative to an equivalent monohull (which was composed of two demihulls with asymmetrical section shapes) the catamaran with symmetrical sections has a resistance reduction of 20–25 percent over a speed range corresponding to Fn = 0.5–1.0. This is shown in Figure 2.

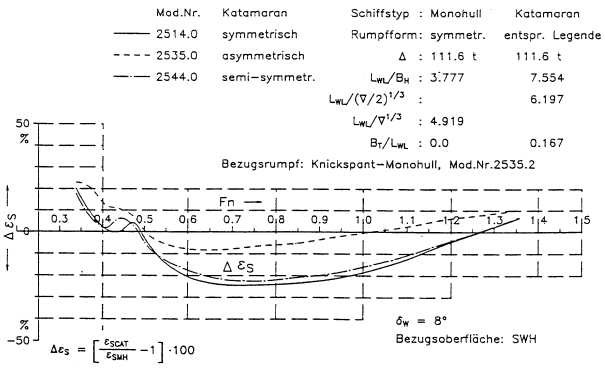

Figure 2 – Resistance test - catamarans compared to the monohull

• The interference resistance due to the presence of a second hull, has its maximum at Fn = 0.45–0.5, the hump speed. The symmetrical form has the largest interference drag of the three section types. However, compared with an equivalent catamaran having the NPL round bilge hull form (Insel and Moland 1992), the symmetric hard chine hull form has remarkably smaller interference drag. This is illustrated in Figure 3.

• The influence of hull spacing is shown in Figure 4. Catamarans having the standard hull spacing of B_T/L_{WL} = 0.167 are compared to a monohull and a catamaran with infinite hull spacing. Below Fn = 0.7 the lowest residuary resistance-to-weight ratio (ε_R) was obtained by a catamaran with infinite hull spacing; while the monohull had higher values of ε_R over the entire speed range.

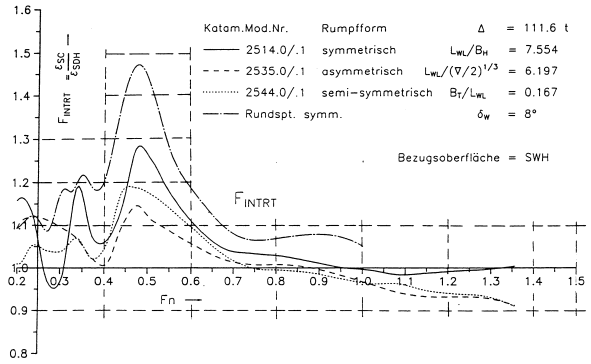

Figure 3 – Interference resistance due to the presence of the second hull

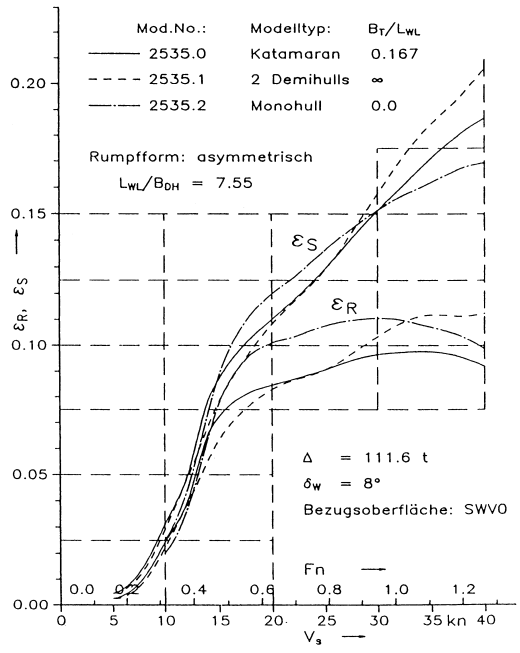

Figure 4 – Interference of hull spacing

b) The propulsion tests of the preliminary Series demonstrated that:

• The symmetrical form had the lowest delivered power and highest propulsive efficiency, while the asymmetrical form had the highest delivered power and lowest propulsive efficiency.

• The semi-symmetrical form had delivered power and propulsive efficiencies similar to those of the symmetric form.

c) The seakeeping tests showed that:

• The seakeeping qualities of the three catamaran types were more affected by the wave length and height, and the wet-deck clearance (above the undisturbed free surface) than by the section symmetry.

• With regard to ride comfort, which is an essential requirement for passenger catamarans, the catamaran with semi-symmetrical sections showed the lowest vertical accelerations at wave heights that were no greater than the wet deck clearance.

• The symmetrical form had vertical accelerations that were 5 to 10 percent greater than the accelerations of the semi-symmetrical form.

• The asymmetrical form had the largest vertical accelerations and the least speed loss.

Selection of the Final Section Symmetry

The preliminary tests clearly demonstrated that the symmetrical form required the lowest propulsive power for speeds corresponding to Fn = 0.7–1.2 (the speed range for which the catamarans are designed). This form also showed acceptable seakeeping qualities at significant wave heights of up to 2.0 m, which prevail in European coastal waters. Consequently, it was decided the VWS Hard Chine Catamaran Series '89 would consist only of forms with symmetric sections, a transom wedge, and external spray rails.

THE LAYOUT OF THE SERIES

Basic Requirements

The series was initially developed for high speed planing catamarans having waterline lengths of 25 to 35 m and carrying 150 to 200 passengers. However, the scope of the series was extended to take into account the following design requirements:

- Hull lengths 20 to 80 m.
- Displacement 25 to 1000 t.
- Service speed 35 to 40 kt, top speed 45 kt.
- The form parameters were selected for best performance at speeds in the range corresponding to $0.8 < Fn < 1.4$.

- Applications were as surveillance craft, passenger and car ferries, and lightweight cargo carriers.
- The form of the afterbody was to be suitable for installation of fully wetted propellers, surface piercing propellers, or water jets.
- The variation of the hull form parameters would be limited to those values which could be realized by full-scale craft.
- The beam-to-draft ratios would be in accordance with the length-to-beam ratios of catamarans suitable for full-scale vessels.

Parent Hull

The parent design of the catamaran series corresponds to a passenger ferry having the following main dimensions:

Length overall	L_{OA}	28.00 m
Breadth overall	B_{OA}	10.50 m
Length of waterline	L_{WL}	23.50 m
Breadth max. at DWL of demihull	B_{XDH}	3.107 m
Draft with deadwood	T	2.310 m
Draft without keel	T_H	1.510 m
Draft of transom	T_{TR}	0.809 m
Displacement	Δ	111.6 t

These corresponds to following principal form parameters:

Length-to-beam ratio	L_{WL}/B_{XDH}	7.55
Slenderness ratio	$L_{WL}/(\nabla/2)^{1/3}$	6.20
Beam-to-draft ratio	B_{XDH}/T_H	2.05
Transom draft-to-hull draft ratio	T_{TR}/T_H	0.54

All hull variations of the series are derived from the geometry of this parent design.

Hull Form Particulars

Length-displacement ratio

The length-displacement ratio of the demihull $L_{WL}/(\nabla/2)^{1/3}$ has the greatest effect on the wave resistance of catamarans. Length-displacement ratio increases with the length-to-beam ratio as shown by Figure 5. A systematic variation of the slenderness ratio at each length-to-beam ratio was omitted to avoid unrealistic beam-to-draft ratios. A variation of 4 percent in the slenderness ratio could be obtained by altering the design displacement by 10 percent.

Length-to-beam ratio

The length-to-beam ratio of the demihulls has the second greatest effect on resistance and propulsion in smooth and rough water. The resistance decreases rapidly with increasing length-to-beam ratio. The waterline length of catamarans grows with increasing length-to-beam ratio if the displacement and the beam-to-draft ratio are held constant. Length-to-beam ratios of L_{WL}/B_{XDH} = 7.55; 9.55; 11.55 and 13.55 were chosen for the catamaran series. The four selected length-to-beam ratios represent the main ranges of value for length, L_{WL} = 10–20 m, L_{WL} = 20–30 m, L_{WL} = 40–50 m and L_{WL} = 60–70 m, respectively.

Because the beam-to-draft ratio was kept nearly constant for the series, the waterline length increased for the fictive hull designs as shown by the following table:

L_{WL}/B_{XDH}	7.55	9.55	11.55	13.55
L_{WL} (m)	23.5	26.7	31.2	36.2

Larger length-to-beam ratios than L_{WL}/B_{XDH} = 13.55, which are of great interest for low wash catamarans, were not included in the series.

Beam-to-draft ratio

Although it does not have a significant effect on the performance of catamarans operating near the planing region, beam-to-draft ratio has a great influence on several particulars of the proposed catamaran series. Because only realistic values of B_{XDH}/T_H were used (Figure 6), an increase of the length-to-beam ratio automatically led to an increase of waterline length. In addition, a large change in draft causes a large shift of the intersection of the chine with the water surface. This can have a disproportionate effect on the resistance.

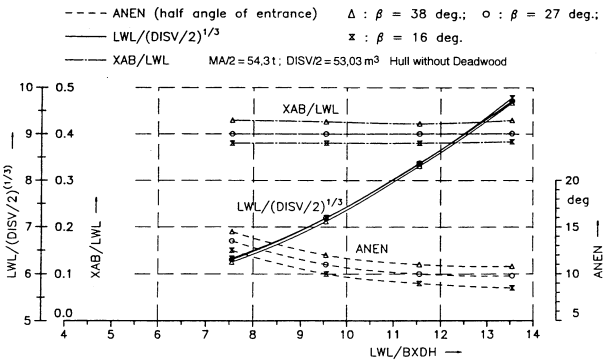

Figure 5 – Length-displacement ratio, waterline entrance angle and LCB position

Transom-draft ratio

The transom-draft, T_{TR} (index "TR" should not be confused with "Trial Condition" used in later sections), which increases with craft speed and which becomes equal to the hull draft in the planing region, should be suitable for installation of the three propulsor types. In the case of the fully wetted propellers, the blades should

not reach below the baseline to protect the propellers against damage by grounding. Consequently, three transom draughts, each best suited for one propulsor type, were chosen:

- $T_{TR}/T_H = 0.54$ This is a standard ratio and is well suited for fully wetted free running propellers.
- $T_{TR}/T_H = 0.68$ This ratio is optimal for free running surface piercing propellers, but also for both propeller types operating in tunnels.
- $T_{TR}/T_H = 0.95$ This ratio is optimal for the installation of waterjets.

Deadrise

The deadrise – its distribution over the length of the hull and the twist or warp of the afterbody bottom – affect the resistance, the powering performance and the seakeeping qualities. Additionally, the magnitude of the deadrise in the afterbody depends to a great extent on the type of propulsor that is to be installed. To determine the effects of deadrise on the resistance and powering performance characteristics of slender planing catamarans, three values of midship deadrise were chosen. Each value is well suited for one of the propulsor types and for one of the transom drafts. In each case the deadrise decreases to $\beta_{TR} = 6°$ at the transom. The chosen midship deadrise angles are:

- $\beta_M = 38°$ This deadrise is used with $T_{TR}/T_H = 0.54$ and results in the greatest warp of the bottom.
- $\beta_M = 27°$ This deadrise is used with $T_{TR}/T_H = 0.68$ and causes a medium warp.
- $\beta_M = 16°$ This deadrise is combined with $T_{TR}/T_H = 0.95$ and results in small warp (almost constant deadrise). This type of afterbody is considered to be optimal for planing speeds and for the application of waterjets.

Transom-beam ratio

A transom beam equal to the maximum waterline breadth, shifts the longitudinal center of buoyancy too far aft (aft of 0.4 L_{WL} from the stern), as has been seen in previous catamaran design studies. For a nearly optimum LCB position of 0.4 to 0.42 L_{WL}, a transom beam ratio of $B_{TR}/B_{XDH} = 0.92$ was chosen (Figure 6).

Waterline entrance angle

The half waterline entrance angle ANEN depends on length-to-beam ratio, length-displacement ratio and the position of the LCB. This angle decreases with increasing length-to-beam ratio as shown by Figure 5. It also decreases with decreasing deadrise β_M.

Form coefficients of demihulls

The form coefficients of the demihulls – midship section coefficient, C_M and block coefficient, C_B – are presented in Figure 7.

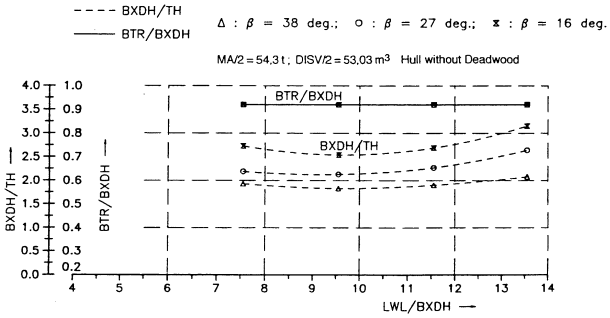

Figure 6 – Beam-to-draft ratio and transom-beam ratio

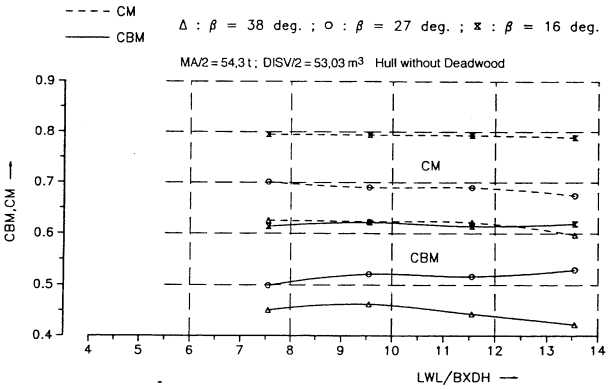

Figure 7 – Form coefficients of demihulls

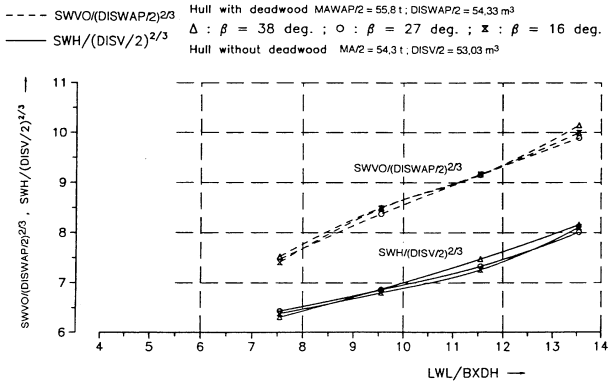

Figure 8 – Wetted surface coefficient of demihulls

LCB-position

The position of the longitudinal center of buoyancy was kept constant for each value of midship deadrise. As shown by Figure 5, with decreasing deadrise, the position of the LCB is shifted aft, from $X_{AB} = 0.42\ L_{WL}$ at $\beta_M = 38°$ to $X_{AB} = 0.4\ L_{WL}$ at $\beta_M = 27°$ and $X_{AB} = 0.38\ L_{WL}$ at $\beta_M = 16°$.

To investigate the effect of shifting LCB forward, designs with an LCB position 2.5% of L_{WL} further forward (denoted as position 2AB) was developed. Three hulls of length-to-beam ratio, L_{WL}/B_{XDH} = 9.55 were designed for X_{AB}/L_{WL} = 0.445 (the afterbody was widened a bit and the forebody was refined). However, this is not a standard LCB position.

Section shape

Small catamarans of 20–30 m length and with service speeds of 35–45 kt are operating just below the planing region, as indicated by the Froude numbers of Fn = 1.0–1.2. The larger catamarans of 40–50 m length are running at even lower Froude number of Fn = 0.9, i.e. in the upper part of the semi-displacement region. Consequently, for Froude numbers of Fn = 0.9–1.2 a hard chine section shape was adopted, since it reduces the resistance by generating hydrodynamic lift and causes separation of the flow.

The standard models have sections that are slightly convex with large deadrise and small flare in the forebody, and waterline entrances that are fine and straight. The afterbodies have a transom with straight buttocks lines and straight sections from about 0.7 L_{WL} aft (measured from the stern). The hard chine is inclined over the whole length.

For increased hull lengths of 60 m and more, the Froude number can drop to Fn = 0.75 or less. At these lower Froude numbers, the hull operates in the middle of the semi-displacement region. Generally, for this condition, round-bilge section shapes have lower resistance than hard chine forms. Therefore, a round-bilge form was included in the program for hulls having medium deadrise. As monohulls with round bilge sections in the forebody and hard chine sections in the afterbody are known for their excellent resistance and seakeeping characteristics, this section combination was chosen for the medium deadrise of the design with the largest length-to-beam ratio. However, the round bilge forms do not belong to the standard hulls that are treated here in more detail.

Section symmetry

As was indicated by the previous investigation, forms with symmetrical section guarantee the lowest resistance at Fn = 0.6–1.2, when compared with an asymmetrical or a semi-symmetrical section form. For this reason, symmetrical sections were chosen for most of the VWS catamaran series. Asymmetrical and semi-symmetrical models with L_{WL}/B_{XDH} = 7.55 were included in the Series.

Gap ratio

The gap ratio B_T/L_{WL}, which is the dimensionless clearance between the demihulls at the waterline, was kept constant for the entire series. The reasons are the following:

- The chosen value of B_T/L_{WL} = 0.167 is an average value for catamarans with hull lengths up to 40.0 m.
- An increase of this value for values of L_{WL}/B_{XDH} < 10, causes an increase in resistance at speeds corresponding to Fn = 0.8–1.2.
- In general, increasing the hull separation to reduce the interference resistance at Fn < 0.6 was not of interest for the planing catamaran series.

Vertical hull clearance ratio

The vertical hull clearance ratio, HCL/L_{WL}, represents the height of the wet deck above the water surface divided by the waterline length. An average HCL/L_{WL} = 0.06 was chosen for the resistance and the propulsion tests. For the seakeeping tests a larger value of HCL/L_{WL} = 0.09 was used. Additionally, this larger HCL/L_{WL} was employed for the low length-to-beam ratios, $L_{WL}/B_{XDH} \leq 9.55$.

Appendages

To investigate the effect of fully wetted and surface piercing propellers on propulsive efficiency and the hull-propulsor interaction coefficients, the following appendages were provided at each demihull:

- All variants (standard configuration, as depicted in Figure 9)
  - One deadwood to carry the tail shaft and to protect the propeller against grounding (deadwood area = 18–20 percent L_{WL}·T).
  - One spade rudder (rudder area = 1.4–1.7 percent L_{WL}·T, NACA 0015 profile).
- All variants with a midship deadrise of $\beta_M = 38°$
  - One inclined shaft with a single arm bracket and one spade rudder.
  - One free running shaft for surface piercing propellers behind the transom with a split inflow flap and one rudder.
- The variants with L_{WL}/B_{XDH} = 7.55 and 9.55 and a midship deadrise $\beta_M = 27°$
  - One tunnel with a height of 20 percent of the fully wetted propeller diameter and one spade rudder.
  - One tunnel with a height of 30 percent of the fully wetted propeller diameter and one spade rudder.
  - One tunnel with a height of 20 percent of a surface piercing propeller diameter with a split inflow flap and a twin spade rudder arrangement.
  - One tunnel with a height of 30 percent of a surface piercing propeller diameter and a twin spade rudder arrangement.

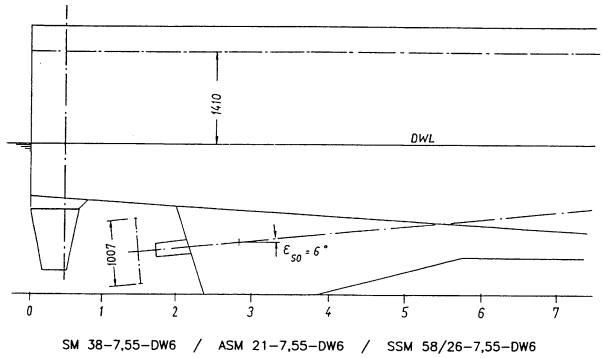

Figure 9 – Transom and deadwood

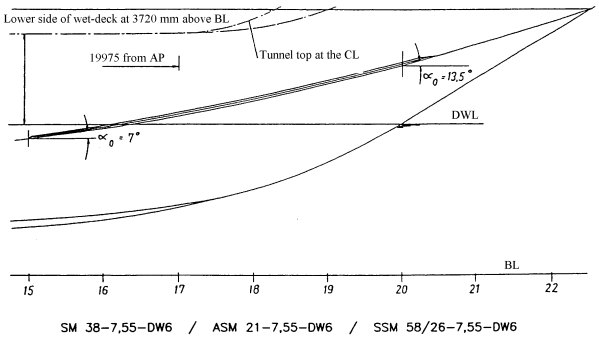

Figure 10 – Stem contour and tunnel top

Propellers

Several propellers were used for propulsion experiments. These were:

- Fixed-pitch propellers (standard configuration)
  D_M = 0.19 m, $P/D_{0.7}$ = 1.4, A_E/A_0 = 1.10, d_B/D = 0.21, Z = 3, cupped trailing edge with modified NACA 16 profile. Note that with this propeller an exceptionally high η_0 = 0.73 was achieved at speed of V = 41 kt.
- Controllable-pitch propellers (two types)
  D_M = 0.16/0.19 m, $P/D_{0.7}$ = 1.0–1.5/0.8–1.6, A_E/A_0 = 0.83/0.77, d_B/D = 0.30/0.29, Z = 4.
- Surface-piercing propellers
  D_M = 0.30 m, $P/D_{0.7}$ = 1.5, A_E/A_0 = 0.66, d_B/D = 0.26, Z = 6.

Transom wedge/flap

Since transom wedges and flaps are the most effective devices to reduce the resistance of slender catamarans, all demihulls were equipped with adjustable transom flaps. Each resistance test was carried out with flap deflections of δ_W = 0°, 4°, 8°, 12°. However, propulsion tests were conducted only for δ_W = 8° (optimal stern wedge angle). The length of the wedges in all cases was 2.8% L_{WL}.

Spray rails

All demihulls were equipped with a spray rail (Figure 10) on both sides of the forebody. These spray rails served to:

- Reduce the wetted area and deck wetness,
- Improve the visibility from the bridge and from the superstructure,
- Prevent spray from climbing up the tunnel sides to the wet deck.

The spray rails are a combination of an integrated and an external one. For a better separation of the spray from the hull, a triangular cross-section was used for the external part of the spray rail. The change in spray rail design parameters over the hull length was chosen according to the results of extensive investigations by the first author (Müller-Graf 1991).

FINAL SCOPE OF THE CATAMARAN SERIES '89

The final scope of the planing catamaran hull Series '89 is presented in Figure 11 (the shaded blocks represent the standard configuration whose resistance and propulsion characteristics are discussed here). Body plans of the standard demihull forms are shown in the Figure 12.

MODEL CONSTRUCTION AND TEST PROCEDURE

A model scale ratio, λ = 7 was chosen for the entire series. This scale ratio avoids tank wall and shallow water effects and guarantees the installation of the model propulsion unit in each demihull, since

$\lambda \geq L_{WLS} / 1.25\, h_{TANK}$, $\lambda \leq L_{WLS} / 0.50\, B_{TANK}$,
$R_{NMIN} \geq 4 \cdot 10^6$ for the hull, $R_{NMIN} \geq 4 \cdot 10^5$ for the propeller.

The models were made of wood and GRP, and had: L_{WL} = 3.66–5.12 m, Δ_M = 274–366 kg and B_T/L_{WL} = 0.167.

Turbulent flow at Reynolds numbers $Rn \leq 2 \cdot 10^6$ was stimulated by square studs, 2.5 x 2.5 mm, by 3 mm high, spaced 25 mm apart and placed on the hulls 0.1 m abaft the stem.

A total of 443 resistance and 132 propulsion tests were carried out in the deep water basin of VWS (dimensions: 240 m x 8 m x 4.8 m) with model speeds of V = 2–11 m/s.

Additional propulsion tests were performed to determine the effects of propeller tunnels with a height of 0.6 D and 0.3 D (60 and 30% of the propeller diameter). The results of these investigations are presented in Müller-Graf (1995).

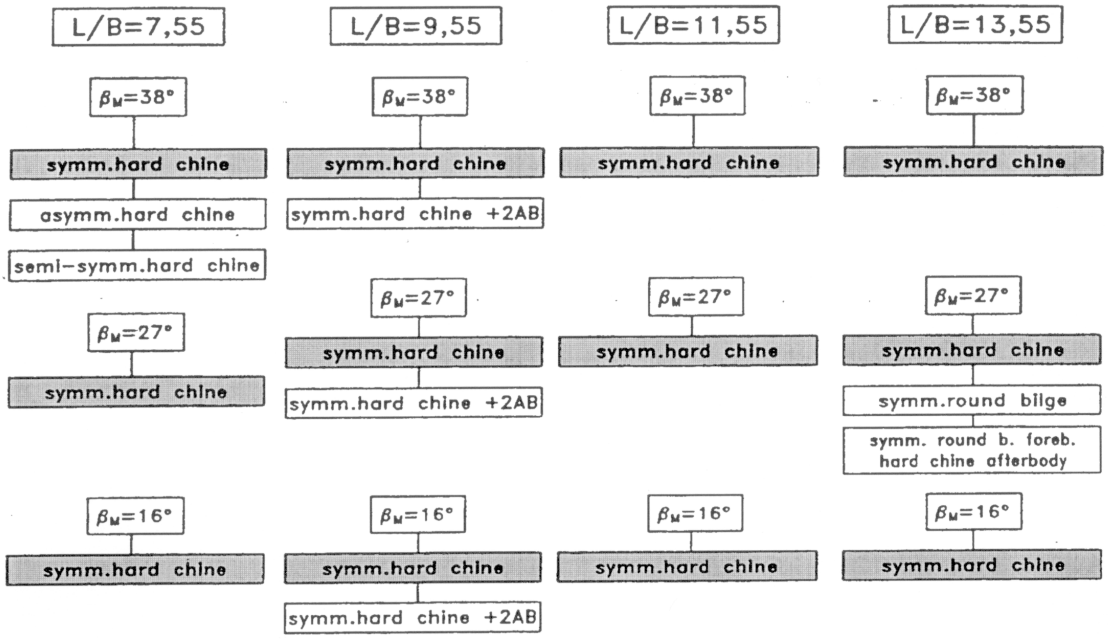

Figure 11 – Scope of the VWS planing hull catamaran Series '89
(shaded blocks indicate standard configuration)

The models were free to trim and heave and were driven (in the standard configuration) by propellers of 0.19 m diameter. The towing force was applied to each demihull at the longitudinal center of gravity and was adjusted for running trim and heave to be in line with the propeller shaft axis. The towing force was measured by means of two resistance dynamometers, one in each hull, as shown in Figure 13.

Because the short measuring times, at model speeds greater than V= 6.5 m/s do not allow adjustment the propeller revolutions so that the required friction deduction or towing force can be obtained exactly, the propulsion tests were performed using a modified "British Method". Under this proceedure, two runs at different thrust-loadings were made for each test speed, and the propeller speeds, forces and torques were interpolated for the correct values.

The VWS test procedure is unique since models are tested under trial condition at a propeller loading which is equal to that of the full-scale vessel. Thus, none of the obsolete speed independent trial allowances had to be applied at the obtained power. Additionally, the full-scale power is corrected for Reynolds number effects on the model propeller. The measured forces and torques were much larger than in other European towing tanks:

- The model resistance was up to 120 kg (1180 N).
- The trust of each model propeller reached values of up to 50 kg (490 N)
- The torque of each model propeller reached value of up to 2.5 kgm (24.5 Nm).
- The rate of rotation of the model propellers reached values of up to 45 s^{-1} (2700 rpm).
- The towing carriage was run at speeds of up to 11 m/s.

RESULTS OF TESTS

The comprehensive resistance and propulsion test results were used to develop a set of design charts for predicting resistance, propulsive efficiency and hull propulsor interaction coefficients under tank and trial conditions. Using these coefficients reliable predictions of the powering performance of fast catamarans can be obtained.

The original experimental results were presented in several formats. One of these was residual resistance-to-weight ratio:

$$\varepsilon_R = (R_{TM} - R_{FM}) / \rho_M \nabla_M g = R_R / \rho_M \nabla_M g$$

Graphically ε_R is given as $\varepsilon_R = f\ (L_{WL}/B_{XDH}, Fn_{\nabla/2}, \beta_M, \delta_W)$, where

L_{WL}/B_{XDH} = 7.55–13.55;
$Fn_{\nabla/2}$ = 4.0/3.5/3.0/2.5/2.0/1.5/1.25/1.00/0.75/0.50;
β_M = 38°/27°/16° and
δ_W = 0°/4°/8°/12°.

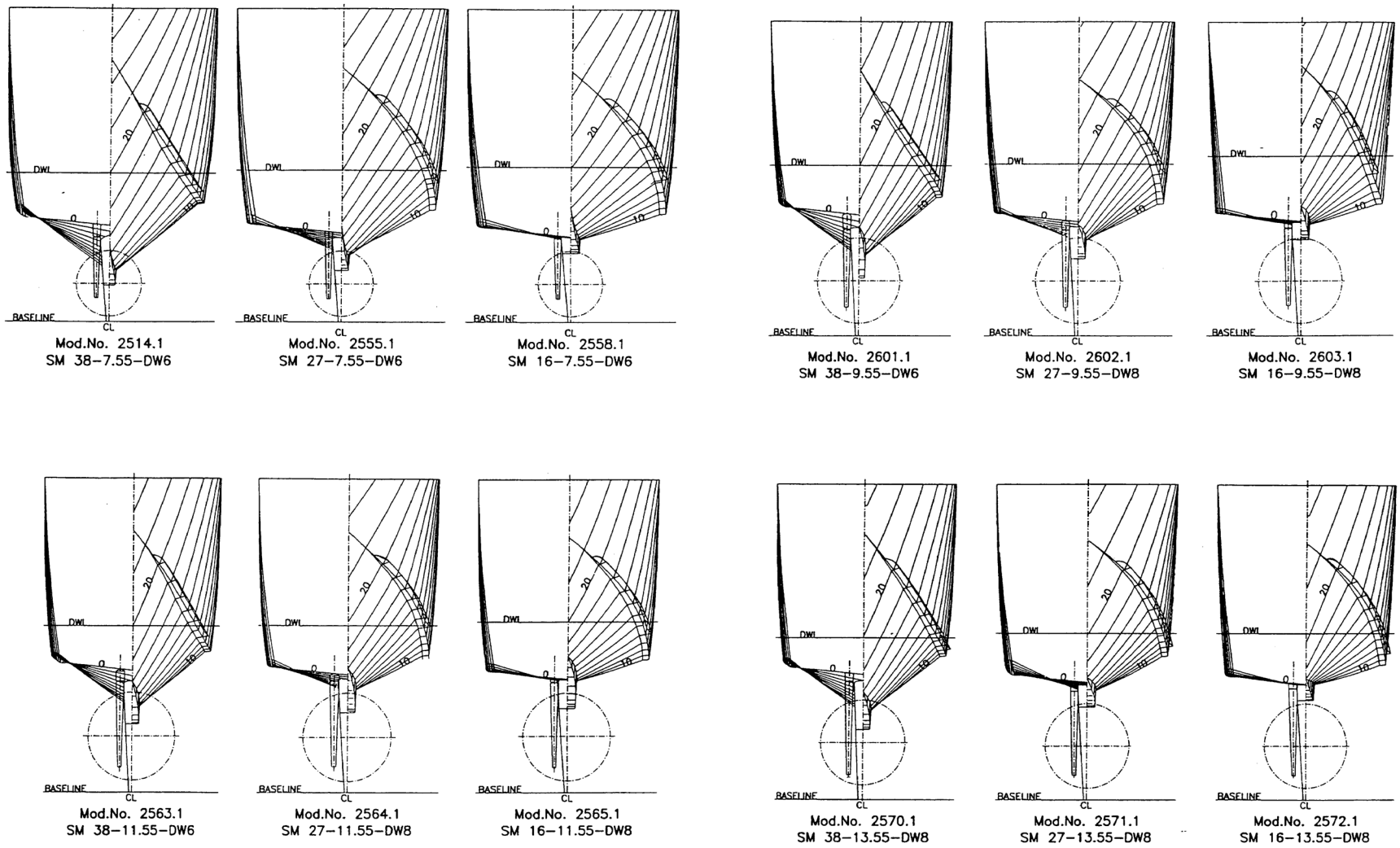

Figure 12 – Section plan of demihulls

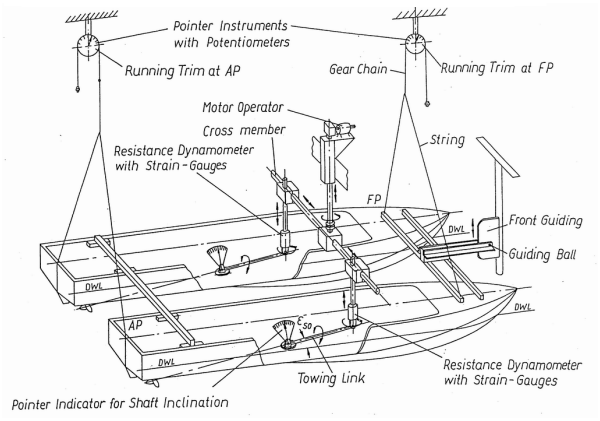

Figure 13 – Towing set-up for catamarans at the VWS with two electric resistance dynamometers

The propulsive efficiency η_D, the hull propeller interaction factors, t_X and w_T, the hull efficiency η_H, and the relative rotative efficiency η_R, are presented in the same functional form as the residuary resistance, except that only one wedge angle, $\delta_W = 8^o$ (which is found to be an optimum value) is presented.

For quick evaluation of installed power, the value of specific power relative to the brake power ε_{BTR} is given for the same values of L_{WL}/B_{XDH}, $Fn_{\nabla/2}$, β_M and $\delta_W = 8^o$ as above. ε_{BTR} based on delivered power, P_{DTR}, corrected for the mechanical losses, η_M, due to gear and propeller shafting, is

$$\varepsilon_{BTR} = P_{DTR} / (\eta_M \Delta g V_S)$$

The specific power, ε_{BTR}, and propulsive coefficients include the effects of the Reynolds number correction on the model propeller.

MATHEMATICAL MODELS

Through the application of regression analysis, three groups of mathematical models, for the reliable evaluation of power, have been derived:

- "Speed-independent" model for the residuary resistance-to-weight ratio of (ε_R).
- "Midship-deadrise-independent" models for the evaluation of dynamic trim, propulsive coefficients and specific power ratio (θ, η_D, η_O, η_H, w_T, t_X and ε_{BTR}).
- Models for wetted surface coefficient and length-to-displacement ratio (WSC and $L_{WL}/(\nabla/2)^{1/3}$).

All three of the regression models are expressed by a single equation of the following form:

$$\mathbf{X} = \sum \text{coeff}_i \cdot Fn_{\nabla/2}{}^{ai} \cdot \beta_M{}^{bi} \cdot \delta_W{}^{ci} \cdot (L_{WL}/B_{XDH})^{di},$$

where

$$\mathbf{X} = (\varepsilon_R,\ 1-t_X,\ \eta_H,\ \theta,\ \eta_D,\ 1-w_T,\ \eta_O,\ \varepsilon_{BTR},\ \text{WSC},\ L_{WL}/(\nabla/2)^{1/3}).$$

The polynomial terms and corresponding coefficients for each equation are given in Tables 3 to 12 of Appendix 1. The terminology used, as for instance "speed-dependant" (and analogous to that "midship-deadrise-independent"), as well as the tools and "tricks" applied in developing the regression models are given in Radojcic (1991), Radojcic and Matic (1997), and Radojcic, et al. (1997, 1999, 2001). The decision not to delve into the development of the regression models is based on the desire to present practical powering prediction formulas for catamaran Series '89 – to concentrate on the catamaran hydrodynamics only – and not to become immersed in the mathematics. Since the general equation given above, along with the polynomial terms and coefficients look daunting, actual examples using the three groups of regression models are given in the Table 1.

An important part of all regression models are the boundaries of applicability that are explicitly given in Table 2. Nevertheless, it must be emphasized that the regression models should only be used to predict the performance of a new hull whose characteristics (including secondary hull form parameters) are similar to those of the data underlying its derivation, i.e. to the catamaran Series '89.

The accuracy and quality of the regression models is depicted in graphical form, Figures 14 to 16, and in statistical form – Appendix 1's Table 3 (at the bottom) and Table 13. The graphical presentation of the errors is important to the naval architect (end user) and the statistical values provide a good measure of model

Table 1 – Application examples for three math model groups

- Residuary drag-weight ratio for $Fn_{\nabla/2} = 2.50$: $\varepsilon_R = -5.538630171 + (-9.917725821) \cdot (L_{WL}/B_{XDH})^{1/2} + \ldots + (-7.85099E\text{-}05) \cdot (\beta_M)^{1/2} \cdot (\delta_W)^1 \cdot (L_{WL}/B_{XDH})^3$
- Quasi propulsive efficiency for $\beta_M = 16°$: $\eta_D = -1697.527857 + (-208.6648087) \cdot (L_{WL}/B_{XDH})^{1/4} + \ldots + 1.275101545 \cdot (Fn_{\nabla/2})^2 \cdot (L_{WL}/B_{XDH})^2$
- Wetted surface coefficient: $WSC = -963.4005565 + 173.5484274 \cdot (L_{WL}/B_{XDH})^{1/2} + \ldots + 6.71128E\text{-}10 \cdot (\beta_M)^4 \cdot (L_{WL}/B_{XDH})^4$

Table 2 – Boundaries of applicability for three math model groups

Mathematical model	Continuous boundaries	Discrete boundaries
ε_R	$L_{WL}/B_{XDH} = (7.55 \div 13.55)$ $\beta_M = (16° \div 38°)$	$Fn_{\nabla/2} = 0.50, 0.75, 1.00, 1.25, 1.50, 2.00, 2.50, 3.00, 3.50, 4.00$ $\delta_W = 0°, 4°, 8°, 12°$
$1\text{-}t_X$, η_H, θ, η_D, $1\text{-}w_T$, η_O, ε_{BTR}	$L_{WL}/B_{XDH} = (7.55 \div 13.55)$ $Fn_{\nabla/2} = (0.75 \div 4.00)$	$\beta_M = 16°, 27°, 38°$ $\delta_W = 8°$
WSC, $L_{WL}/(DISV/2)^{1/3}$	$L_{WL}/B_{XDH} = (7.55 \div 13.55)$	$\beta_M = 16°, 27°, 38°$

validity. Predictions using all of the derived regression models are shown in Figure 17. The absence of instabilities between the points used to derive the regression models is shown in Figures 20 and 24, as well as in Figures 14 to 17.

EVALUATION PROCEDURE

The performance evaluation procedure, adopted by VWS Berlin, is described below.

Total Resistance

Total resistance (with appendages) for towing tank conditions is obtained from

$$R_{TTK} = R_R + R_F$$

for volume Froude numbers (based on a demihull)

$$Fn_{\nabla/2} = V / (g\,(\nabla/2)^{1/3}) = 0.5\text{–}4.0.$$

Here

$$R_R = \varepsilon_R\, \rho_S\, \nabla_S\, g$$

and

$$R_F = 0.5\, \rho_S\, (C_F + \Delta C_F)\, 2\, S\, V_S^2,$$

where

$C_{F(ITTC\text{-}1957)} = 0.075 / (\log Rn - 2)^2$ and $\Delta C_F = 0.3 \cdot 10^{-3}$.

S (or SWVO) is wetted surface with deadwood and rudder. Consequently, the total resistance at towing tank condition is

$$R_{TTK} = \varepsilon_R\, \rho_S\, \nabla_S\, g + 0.5\, \rho_S\, (C_F + \Delta C_F)\, 2\, S\, V_S^2 \quad [kN]$$

Hull Propulsor Interaction Coefficients at Tral Conditions

The hull propulsor interaction coefficients are the components of the propulsive efficiency. They are indispensable in powering performance predictions based on conventional resistance predictions.

Propulsive efficiency (η_D)

At trial conditions the propulsive efficiency (or quasi-propulsive efficiency), η_D, is defined as

$$\eta_D = P_{ETR} / P_{DTR},$$

where

$P_{ETR} = R_{TTR}\, V$	[kW]	Effective power at trial condition
R_{TTR}	[kN]	Sum of the hydrodynamic and aerodynamic resistance components under trial condition
P_{DTR}	[kW]	Delivered power at trial condition.

η_D is composed of three main components

$$\eta_D = \eta_0{}^*\, \eta_H\, \eta_R$$

which include four subcomponents

$$\eta_D = \eta_0\, F_{RN}\, [(1 - t_\Psi)/(1 - w_T)]\, (\eta_B/\eta_0)$$

$\eta_0{}^*$ Reynolds number effects corrected open water efficiency of the model propeller under trial conditions (explained in the Powering Predictions, Trial Conditions section)

η_H Hull efficiency under trial conditions (for inclined shaft)

η_R Relative rotative efficiency under trial conditions

η_B Propeller efficiency behind the hull

F_{RN} Reynolds number correction factor for model-scale to full-scale open water propeller efficiency.

Propeller efficiency (η_0)

The open water propeller efficiency is the largest component of the propulsive efficiency. In the present case η_{0TR} is determined for the trial condition, based on open water test results either for a systematic propeller series or an appropriate propeller design. At present, a

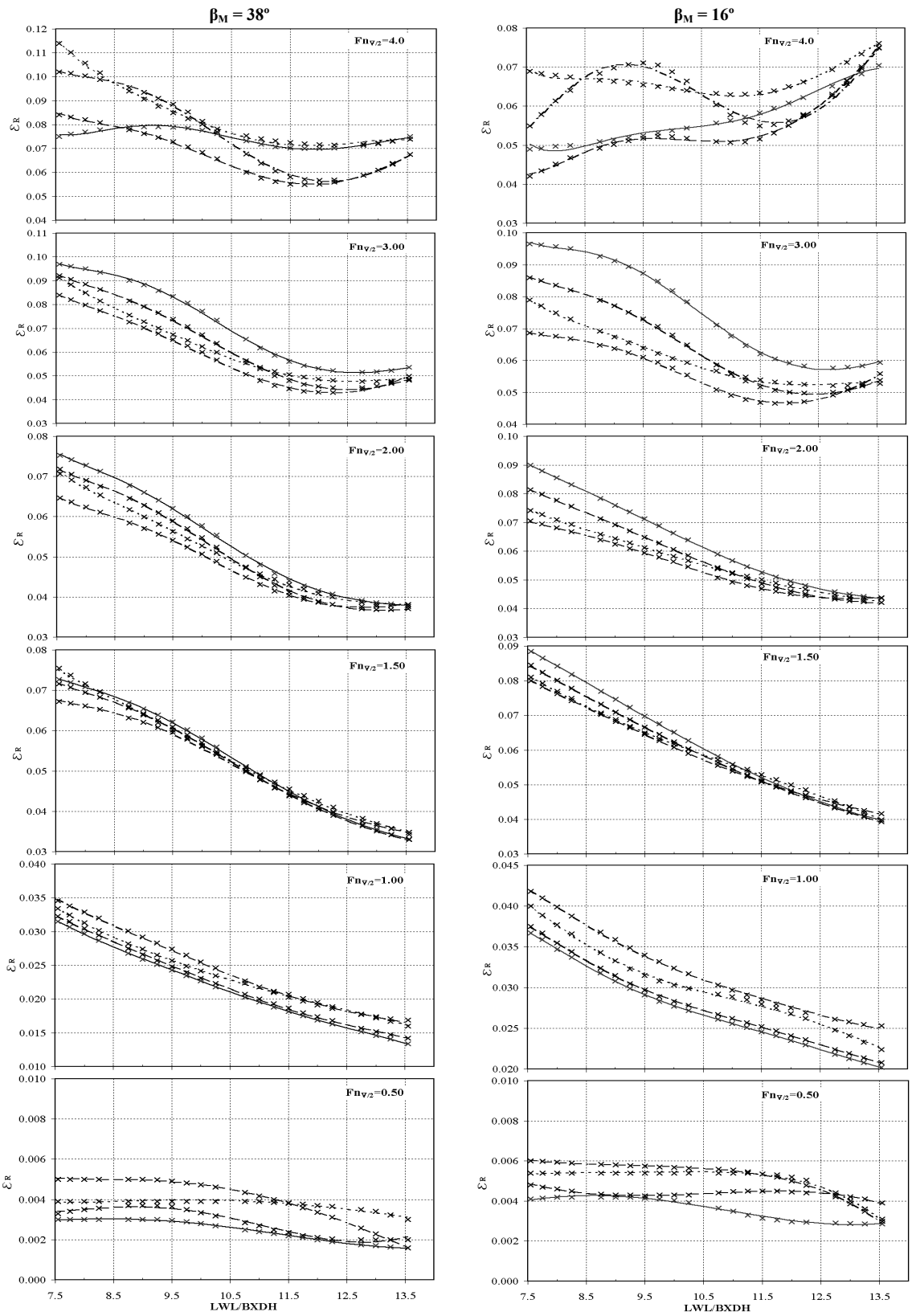

Figure 14 – Drag-weight ratio of the residual resistance, $\varepsilon_R = f(L_{WL}/B_{XDH}, \delta_W)$ given for different values of $Fn_{\nabla/2}$ and $\beta_M = 16^o$ and 38^o (dots are original VWS values while lines are calculated values)
—— $\delta_W = 0^o$, - - - $\delta_W = 4^o$, ····· $\delta_W = 8^o$, —·— $\delta_W = 12^o$

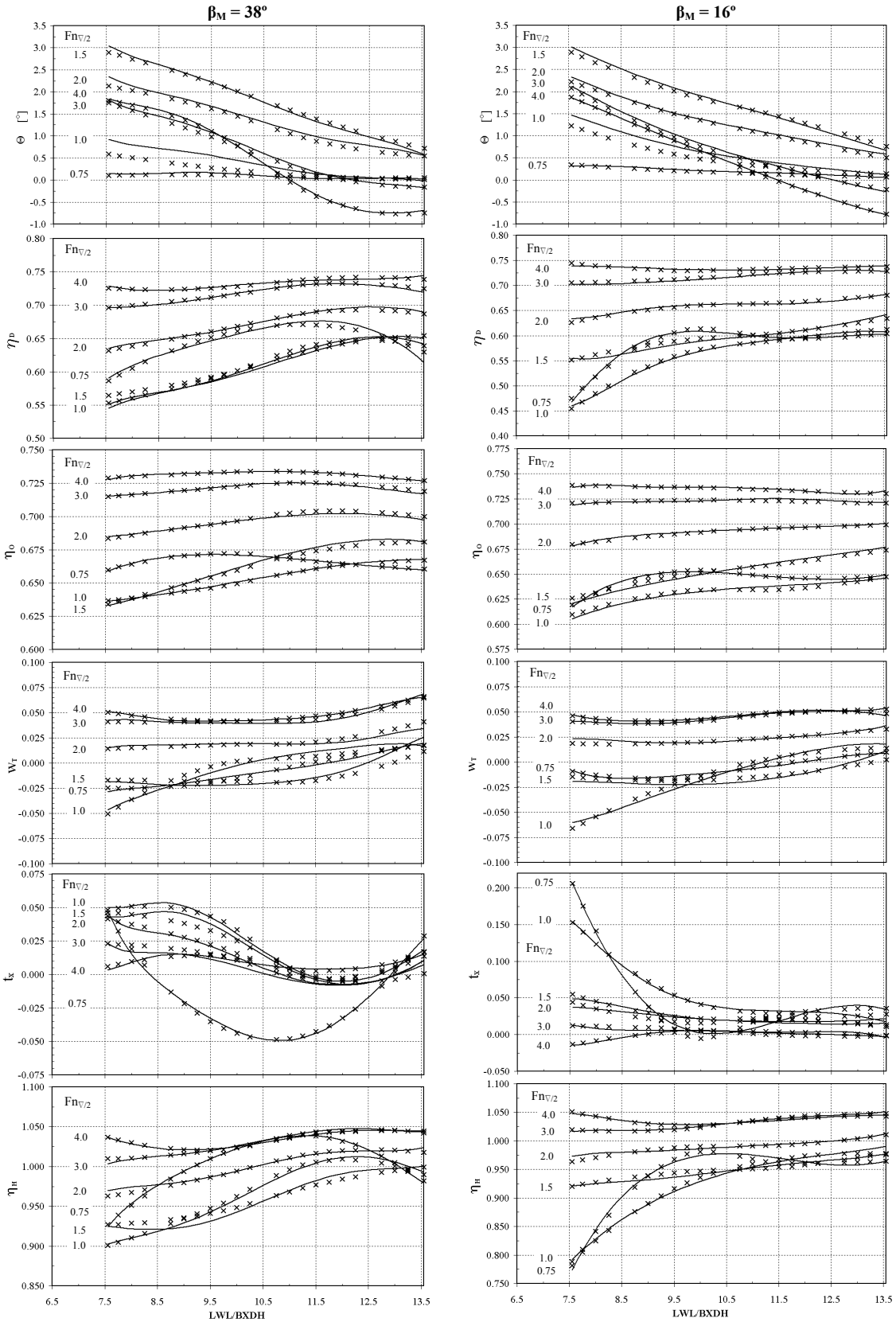

Figure 15 – Trim θ and propulsive coefficients η_D, η_O, w_T, t_X and η_H given as a f(L_{WL}/B_{XDH}, $Fn_{\nabla/2}$) for $\beta_M = 16^o$ and 38^o, and $\delta_W=8^o$ (dots are original VWS values, lines are calculated values)

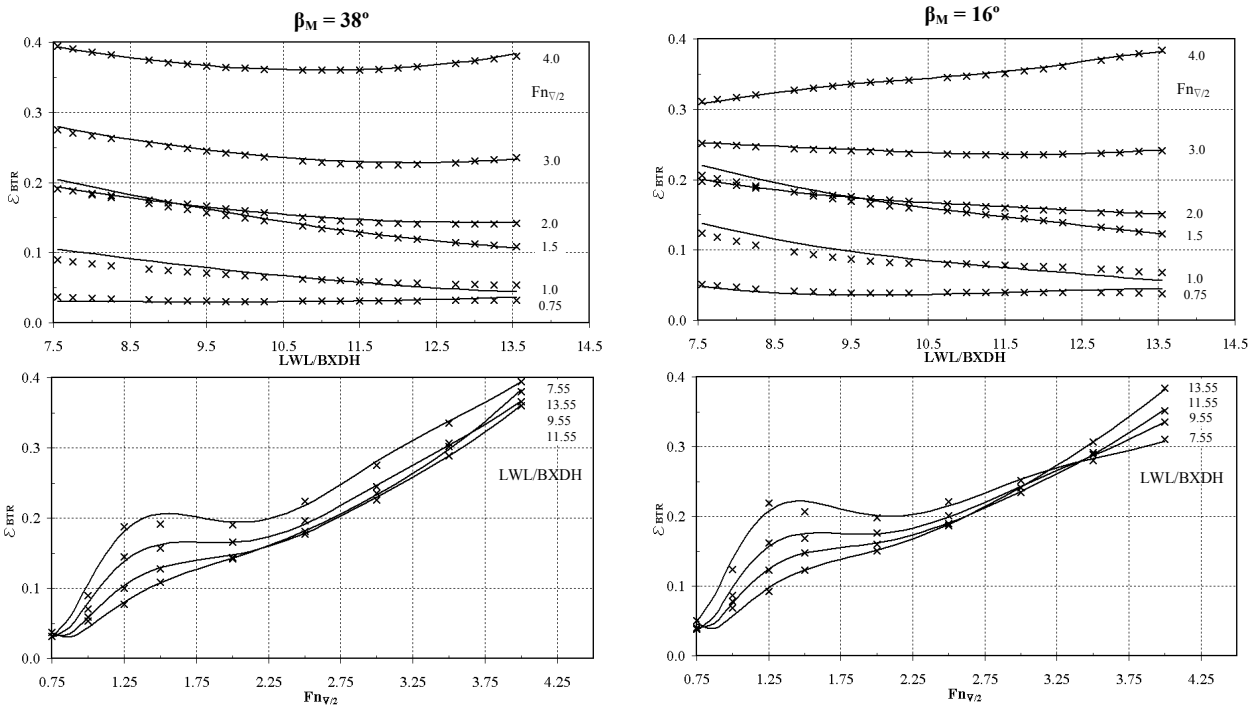

Figure 16 – Specific power $\varepsilon_{BTR} = f(L_{WL}/B_{XDH}, Fn_{\nabla/2})$ and $\varepsilon_{BTR} = f(Fn_{\nabla/2}, L_{WL}/B_{XDH})$ for $\beta_M = 16^o$ and 38^o, and $\delta_W=8^o$ (dots are original VWS values, lines are calculated values)

systematic high speed propeller series that has modern blade section profiles with cuped trailing edges and that takes into account the effects of oblique inflow conditions $\psi = 6–12°$, and the low cavitation numbers typical of high speed vessels, does not exist. In most cases the designer is dependant on the (old) Gawn-Burill Propeller Series having circular arc blade profiles and somewhat lower propeller efficiencies (see for instance Radojcic 1988).

Thrust which should be achieved by each propeller follows from

$$T_{TR\psi} = R_{TTR} / (N_{PR} (1 - t_X)\cos\psi)$$

so that thrust coefficient is

$$K_T/J^2 = R_{TTR} / [\rho_S D_S^2 V^2 (1 - w_T)^2 (1 - t_X)\cos\psi N_{PR}]$$

while, $\sigma_0 = 0.6–0.4$ for $V_S = 39–45$ kt.

Thrust deductiuon factor (t_X)

The trust deduction factor indicates the change of hull resistance due to the working propeller. In the present case it is based on the horizontal thrust component under trial conditions:

$$t_X = 1 - (R_{TTR,M} / \Sigma T_{XTR,M})$$

respectively

$$t_X = 1 - (R_{TTR,M} / \Sigma T_{\psi TR,M} \cos\psi).$$

Trial resistance of the model is

$$R_{TTR,M} = R_{TM} + [(R_{AA,S} + R_{PAR,S} + \Delta R_{AW,S}) / (\lambda^3 \rho_S)]\rho_M.$$

R_{TM}	[N]	Model resistance under tank conditions
$T_{XTR,M}$	[N]	Horizontal thrust component under trial condition
$T_{\psi TR,M}$	[N]	Axial thrust under trial condition
ψ	[°]	Shaft inclination underway relative to horizontal - $\psi = \varepsilon_{S0} + \theta$
ε_{S0}	[°]	Shaft inclination at rest relative to horizontal
θ	[°]	Running trim
λ		Scale ratio.

$R_{AA,S}$, $R_{PAR,S}$, $\Delta R_{AW,S}$ are drag components of the trial conditions (given in the Powering Predictions, Trial Conditions section).

Wake fraction (w_T)

The effective wake fraction of the model is determined on the basis of the open water propeller characteristics by means of the thrust identity at the trial condition and is given by

$$w_T = 1 - (V_{AM}/V_M) = 1 - (J_{TTR,M}\, n_M\, D_M) / V_M$$

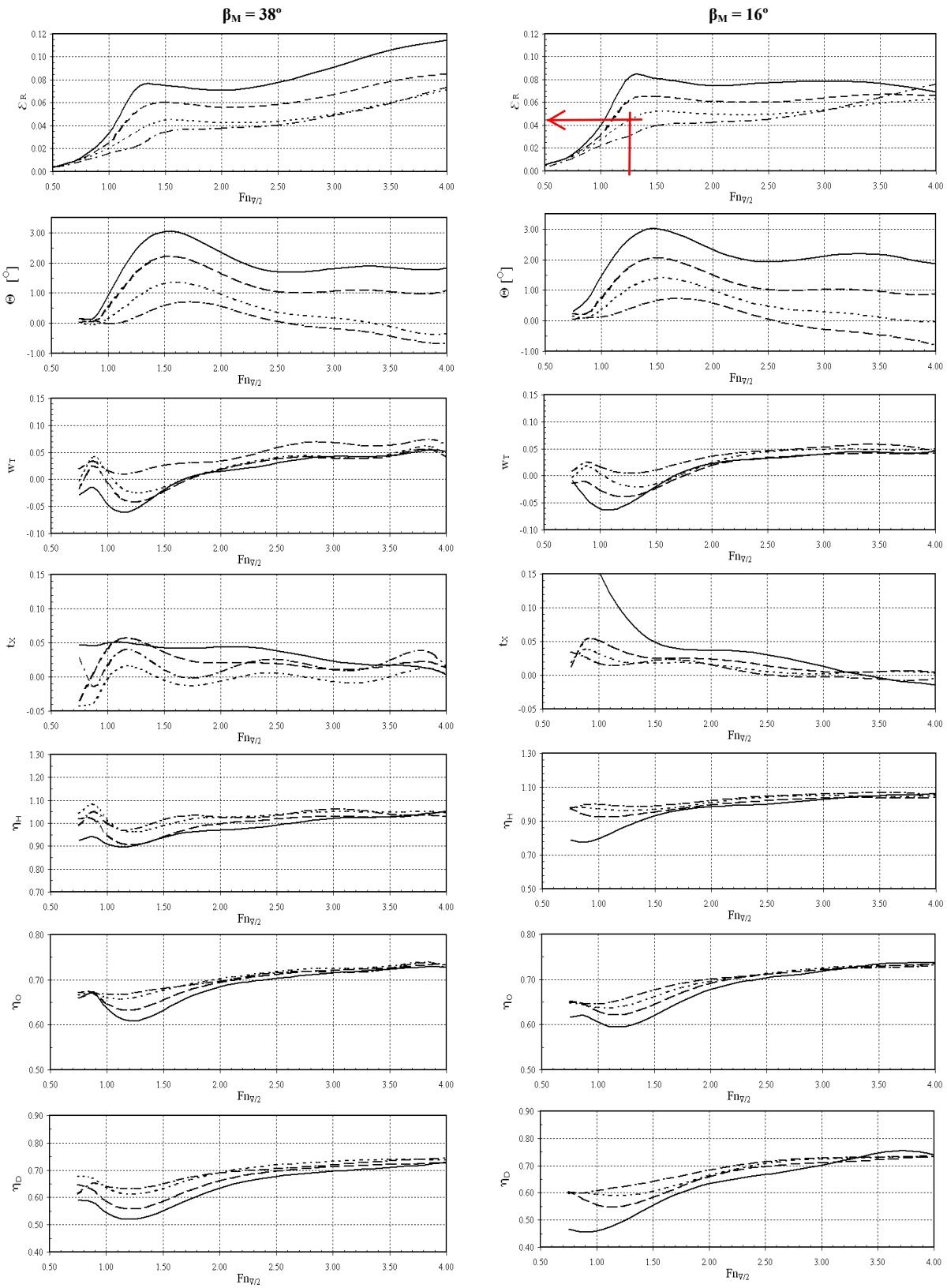

Figure 17 – ε_R, θ, w_T, t_X, η_H, η_O, η_D = f($Fn_{\nabla/2}$, L_{WL}/B_{XDH}) for β_M = 16° and 38°, and δ_W=8°

LWL/BXDH: —— 7.55 – – – 9.55 ····· 11.55 –·–·– 13.55

V_{AM} [m/s] Advance speed of the model propeller at the axial inflow condition determined from the thrust identity

$J_{TTR,M}$ Advance ratio at axial inflow condition determined from thrust identity under trial condition

n_M [s^{-1}] Rate of rotation of the model propeller

D_M [m] Diameter of model propeller.

Hull efficiency (η_H)

The hull efficiency is defined by the ratio $(1–t_X)/(1–w_T)$. However, here, η_H takes into account shaft inclination Ψ. Consequently

$$\eta_H = \eta_{H\Psi} = (1 - t_\Psi)/(1 - w_T)$$

Obviously, $t_\Psi \neq t_X$. If needed, t_Ψ may be obtained from above-mentioned relationship.

Relative rotative efficiency (η_R)

The relative rotative efficiency is caused by the inhomogeneous and oblique inflow conditions at the propeller and by the effects of the rudder on the propeller characteristics. η_R is defined as the ratio of the propeller efficiency in the "behind condition" to that "in open water" and is given by $\eta_R=\eta_B/\eta_0$. Propeller efficiency behind the hull is

$$\eta_B = T_{\psi TR,S}\, V_A / P_{DTR} = T_{\psi TR,S}\, V_A / (2\pi\, n\, Q_{TR})$$

P_{DTR} [kW] Delivered power under trial conditions

Q_{TR} [Nm] Propeller torque under trial conditions

Relative rotative efficiency, η_R, has an almost constant value. So $\eta_R = 0.96$ was adopted throughout.

POWER PREDICTION

Trial Conditions

The powering performance and the propulsive coefficients were determined for the trial condition. At the trial condition, the model propeller works at the same thrust loading as the full-scale propeller. Therefore, the following drag components of the trial condition (which cannot be simulated at the model tests) were taken into account:

$R_{AA,S}$ [kN] Air and wind resistance of the full-scale vessel

$R_{PAR,S}$ [kN] Parasitic drag due to the zink-anodes and the inlet and outlet openings at the bottom of the hull for cooling and sanitary water

$\Delta R_{AW,S}$ [kN] The added resistance in waves at the trials due to rippling seas,

where $R_{AA,S} = C_{AA}\, 0.5\, \rho_A\, (V_S + V_W)^2\, A_V$

$\rho_A = 1.226\cdot10^{-3}$ [t/m^3] Mass density of air

$C_{AA} = 0.65$ Air allowance coefficient

V_S [m/s] Ship speed

$V_W = 3.34$ [m/s] Wind speed for Bn=2

$A_V = 98.5$ [m^2] Projected above-water transverse area

$$R_{PAR,S} = 0.5\, \rho_S\, V_S^2\, [C_{DP}\, (A_{FZ} + A_X)]$$

$C_{DP} = 0.15$

$A_{FZ} = 0.075\cdot0.05\cdot16 = 0.06$ m^2 area of zink anodes

$A_X = 0.20\cdot0.245\cdot2 = 0.098$ m^2 two hull openings

$C_{DP}\, (A_{FZ} + A_X) = 0.0237$ m^2

$\Delta R_{AW,S} = 0.02\, R_{TTK,}$ (2% of R_{TTK} for wind of Bn=2).

Consequently, the total resistance under trial conditions is

$$R_{TTR} = R_{TTK} + R_{AA} + R_{PAR} + R_{AW} \quad [kN]$$

Full-scale trial power and RPM determined by this procedure do not need any other empirical allowances or corrections, except that of the Reynolds number corection for viscous scale effects on the model propeller. The Reynolds numbers of the full scale propellers are larger by at least a factor 10 than those of the model propellers, thus the required torque becomes comparatively smaller. This effect increases the propeller efficiency and decreases the required power. The Reynolds correction for power and rate of rotation is determined by the method of "equivalent profiles" and dependes on propeller diameter, rate of rotation and blade area ratio. For Series '89 the increase of the propeller efficiency amounts to F_{RN} = 1.03–1.07 corresponding to D = 1.0–1.4 m. Typically,

$$F_{RN} = \eta_0^*/\eta_0 = 1.04,$$

where

η_0^* Reynolds number effects corrected open water efficiency of the model propeller

η_0 open water efficiency of the model propeller.

Powering Predicton Methods

As is indicated in Figure 18, powering predictions may be performed for an actual propeller or for any other new (installed) propeller. If an actual propeller is considered, two approaches are available: a conventional method and a short method. Other than the method depicted in Figure 18, powering predictions for any installed propeller may be performed by increasing the power obtained with an actual propeller by a quantity corresponding to the difference between open water efficiency $\eta_{0,\,ACTUAL}$ and $\eta_{0,\,INSTALLED}$.

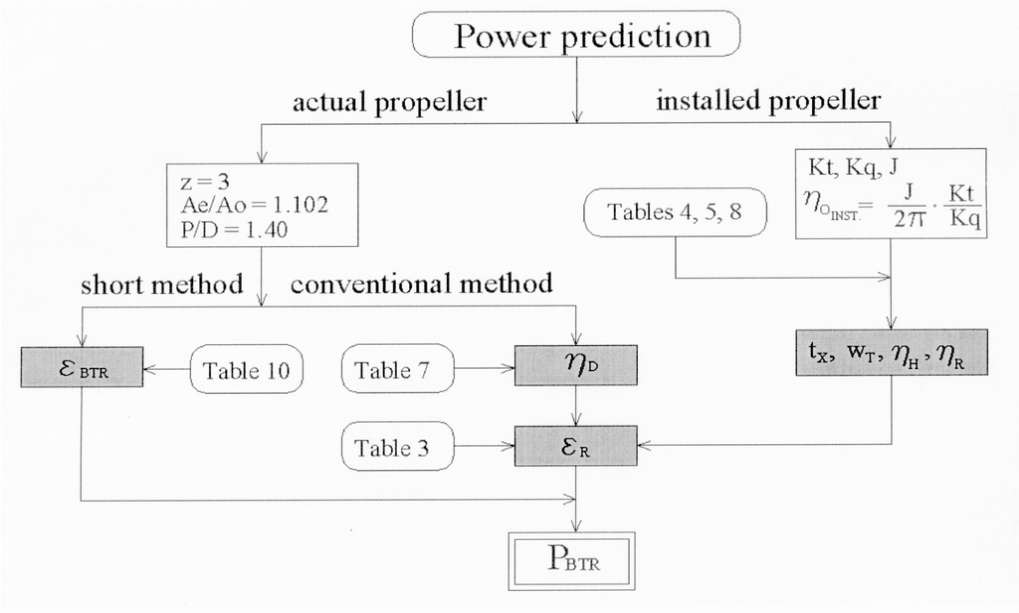

Figure 18 – Algorithm showing the evaluation of power prediction
(shaded blocks indicate values which are calculated by math model)

Conventional Method

The conventional method follows from everything written up till now, i.e.

$$P_{ETR} = R_{TTR}\, V_S \quad \text{and} \quad P_{DTR} = P_{ETR}/\eta_D \quad [kW]$$

$$P_{BTR} = P_{DTR}/\eta_M \quad [kW]$$

where $\eta_M = \eta_G\, \eta_{SH} = 0.94$

$\eta_G = 0.96$ – gear losses and $\eta_{SH} = 0.98$ – shaft losses.

Short Evaluation Method

The short method for brake power evaluation is based on the specific brake power for trial conditions ε_{BTR}

$$P_{BTR} = \varepsilon_{BTR}\, \Delta_S\, g\, V_S \quad [kW]$$

As mentioned earlier, ε_{BTR} includes the effects the Reynolds number correction of the model propeller.

All regression models presented are independently derived. So, a good check of the model quality is to compare independently derived P_{BTR} by using the conventional and short evaluation methods. Detailed algorithms for both procedures is given in Figure 19. Figure 20 shows the final results obtained by each method.

MAIN CHARACTERISTICS OF THE RESISTANCE AND PROPULSIVE COEFFICIENTS

The main characteristics of the resistance and hull-propulsor interaction coefficients of the standard catamaran configuration, as functions of speed and hull form parameters, are described in the following statements:

- The effect of the length-to-beam ratio on the interference resistance is largest for the smallest length-to-beam ratio, $L_{WL}/B_{XDH} = 7.55$ and smallest for the largest, $L_{WL}/B_{XDH} = 13.55$, see Fig. 21.
- The midship deadrise does not have a significant influence on the interference resistance. The smallest deadrise, $\beta_M = 16^o$ causes the least interference resistance, see Fig. 22.
- The transom wedge in combination with an external spray rail was shown to be very effective in reducing both the wave resistance and the frictional resistance. The lift from the wedge decreases the running trim and by this the wave resistance. The spray rail reduces the frictional resistance. For the optimal wedge inclination, $\delta_W = 8^o$, the catamaran with the smallest length-to-beam ratio has the largest reduction in resistance (and vice versa), see Fig. 23.
- Thrust deduction factor, t_X reaches its maximum values ($t_X > 0.1$) in the hump speed region and decreases and holds steady at $t_X < 0.05$ for $Fn_{\nabla/2} > 1.5$–2.0. With an increase in L/B, t_X decreases slightly over the whole speed range, see the 3-D diagram showing t_X in Fig. 24.
- The speed dependence of wake fraction, w_T is exactly opposite to that of t_X. Above the hump region it increases with speed and holds steady at around 0.05 above $Fn_{\nabla/2} = 2.5$ (depending on L/B ratio, lower L/B

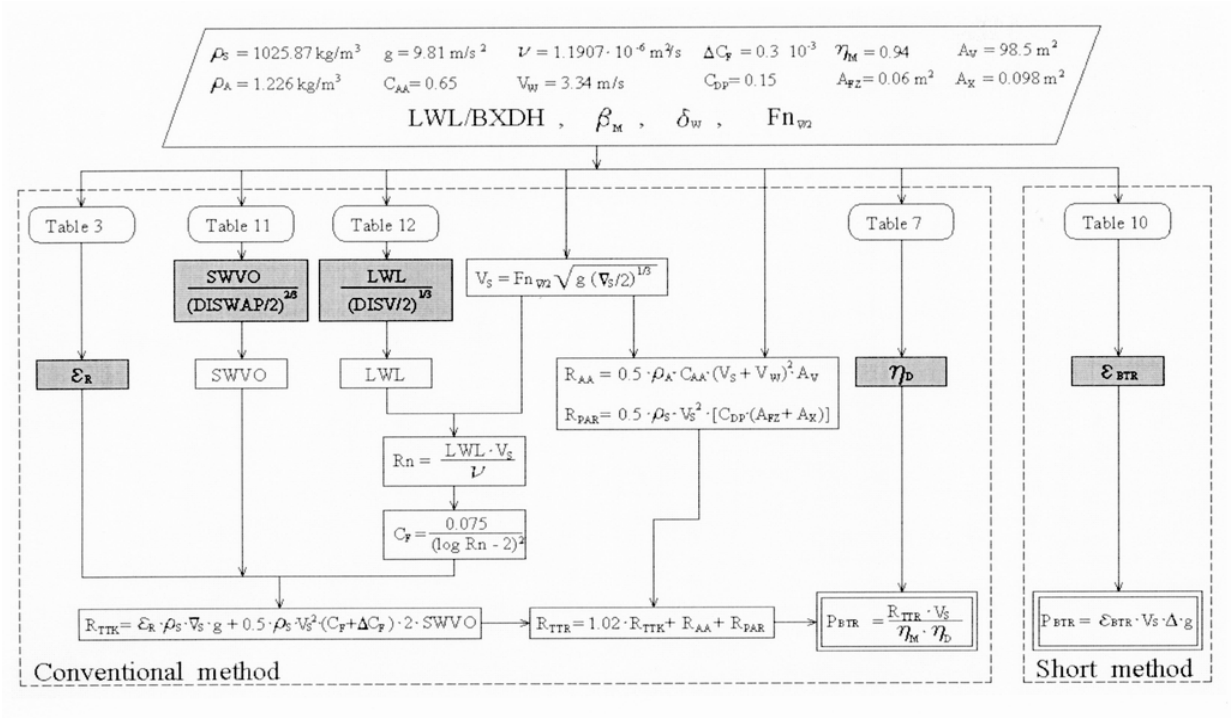

Figure 19 – Algorithm showing evaluation procedure for obtaining P_{BTR}
(shaded blocks indicate values which are calculated by math model)

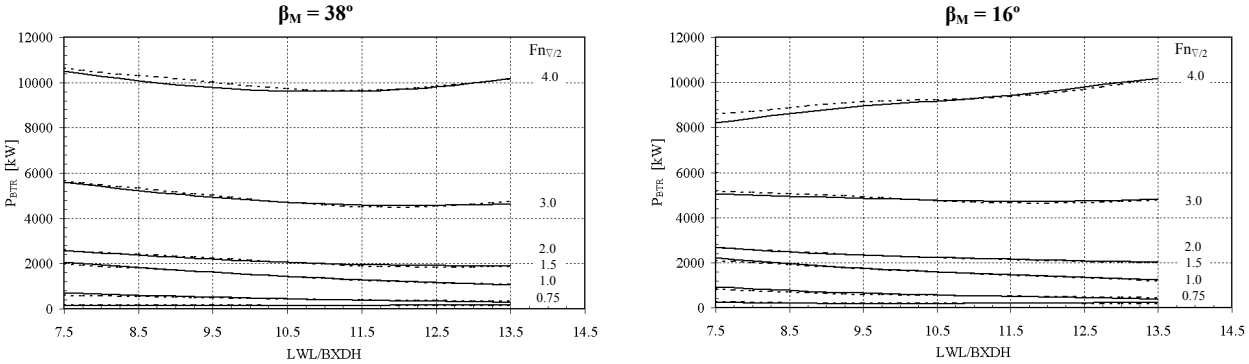

Figure 20 – $P_{BTR} = f(L_{WL}/B_{XDH}, Fn_{\nabla/2})$ for $\beta_M = 38^o$ and 16^o, and $\delta_W = 8^o$, calculated by conventional (·····) and short (——) method ($\Delta = 111.6$ t, $z = 3$, $A_e/A_o = 1.1$ and $P/D = 1.4$)

ratios correspond to slightly lower w_T), see the 3-D diagram showing w_T in Fig. 24.

- Because it is a function of t_X and w_T, the hull efficiency η_H oscillates at lower speeds. Above $Fn_{\nabla/2} = 2.0–2.5$ it holds steady in the range $\eta_H \approx 1.02–1.03$, depending on the L/B ratio and β_M.
- The relative rotative efficiency η_R shows small oscillations around hump speed (depending weakly on L/B ratio) and holds steady at 0.96–0.98 above $Fn_{\nabla/2} = 1.0–1.5$.
- Propeller efficiencies (η_O and η_B) reflect the effect of thrust loading, particularly at the hump speed. Both efficiencies increase gradually from $Fn_{\nabla/2} = 1.3$ to their highest values of $\eta_O = 0.73$ and $\eta_B = 0.70$ for speeds of around 40 kt ($Fn_{\nabla/2} = 3.5–4.0$).
- Propulsive efficiency η_D depends on the thrust loading and tracks the propeller efficiency. The lowest values arise in the hump speed region where $\eta_D = 0.45–0.65$ (higher values correspond to higher L/B ratios). Propulsive efficiency increases gradually to an exceptionally high $\eta_D = 0.72–0.73$ for $Fn_{\nabla/2} = 3.5–4.0$ (40 kt), see the 3-D diagram showing η_D in Fig. 24.

It should be noted, however, that the main characteristics of resistance (actually ε_R), dynamic trim, and propulsive coefficients are also given in Fig. 17.

NON-STANDARD CONDITIONS AND CONFIGURATIONS

The standard conditions and the configurations that are treated by the regression models are given in the Mathematical Models section and are explained in the Powering Prediction and Layout of the Series, and Final Scope of the Series '89 Catamarans sections, respectively. Nevertheless, the influence of non-standard conditions and configurations on the final result – Delivered Power – is briefly depicted graphically in Appendix 2.

The influence of Reynolds number corrections and trial condition allowances are illustrated in Figures 25 and 26 respectively. The influence of section shape is shown in Figures 27 and 28, while the effect of change of longitudinal center of buoyancy LCB ("Symm. Hard Chine + 2AB" as denoted in Figure 11) is shown in Figure 29. The impact of varying propulsor types and appendage configurations are depicted in Figures 30–32.

CONCLUDING REMARKS

A novel and reliable method for predicting the propulsive power of high-speed catamarans is presented. The residual resistance, as well as the components of the propulsive efficiency that are needed for reliable evaluation of delivered power, may be determined from the regression models. The regression models are based on multiple linear regression analysis of the large number of propulsion data from the VWS hard chine catamaran Series '89.

The powering prediction method is reliable because the propulsive coefficients for Series '89 were obtained from self-propulsion tests under trial conditions. Under these test conditions the model propellers are working at a loading which is equal to that of the full-scale propellers. Therefore, none of the obsolete (speed independent) trial allowances for power and RPM have to be applied to the power obtained by these regression models.

This powering prediction method replaces a large stock of data, concerning resistance, running trim and propulsive coefficients. The method allows optimization of the hull-form parameters and prediction of powering in early design stage for catamarans having length-to-beam ratios of L_{WL}/B_{XDH} = 7.55 to 13.55 and midship deadrise values of β_M = 16° to 38° with an optimal wedge inclination of δ_W = 8°. Residuary resistance and hull-propeller interaction coefficients versus speed are given for a large speed range – from the hump speed to planing speeds (up to $Fn_{\nabla/2}$ = 4, $Fn_L \approx 1.5$).

Moreover, since the propulsive coefficients are more influenced by length-to-beam ratio than by section shape, these regression models may be used relatively successfully for other catamaran forms (series). So, powering predictions for round bilge hull forms is possible if accurate resistance characteristics are available.

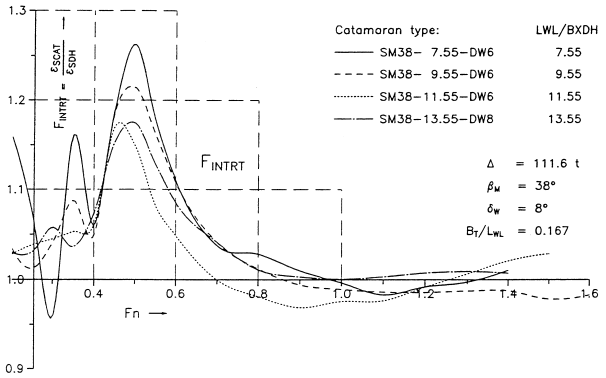

Figure 21 – The effect of length to beam ratio on the interference resistance

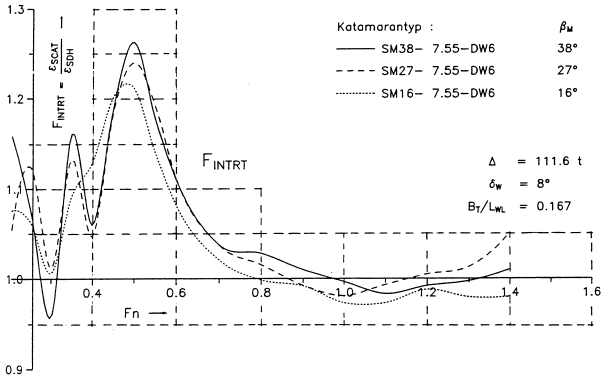

Figure 22 – The effect of midship deadrise on the interference resistance

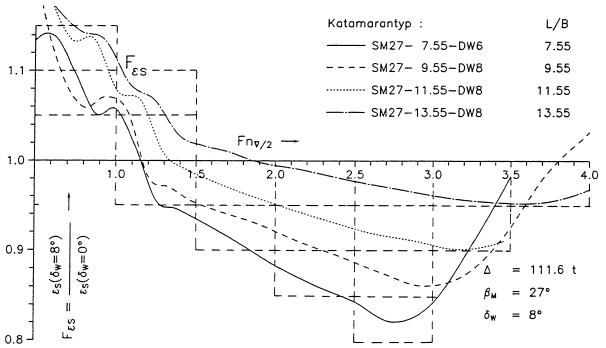

Figure 23 – The influence of transom wedge on resistance

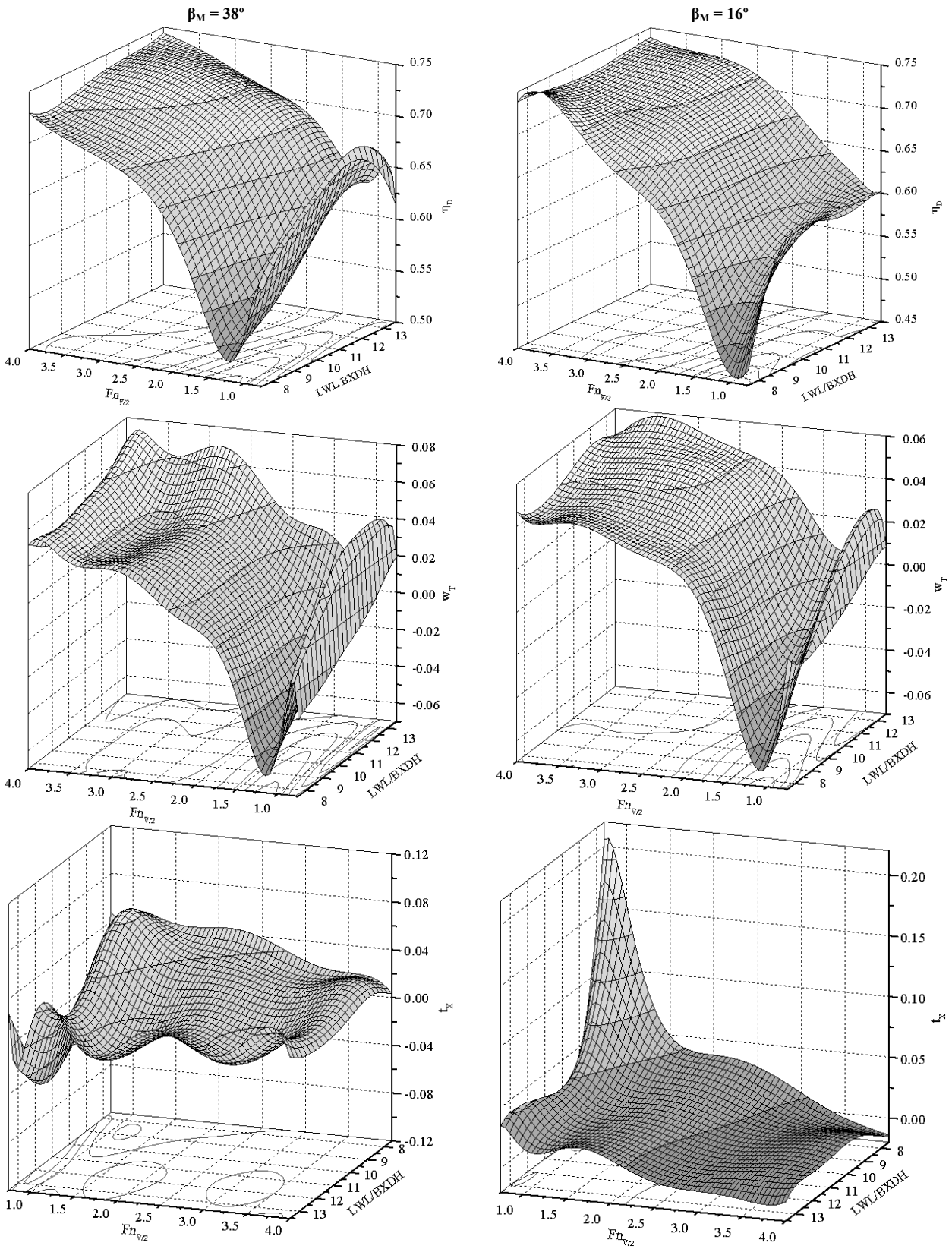

Figure 24 – 3D diagrams showing characteristics of η_D, w_T and t_X as a f($Fn_{\nabla/2}$, L_{WL}/B_{XDH}) for β_M=16° and 38°, and δ_W=8°

REFERENCES

Clement, E. P. 1962. Graphs for Predicting the High Speed Resistance of Planing Catamarans. *Internat. Shipbuild. Progress*, **9**(99):464–77.

Fry, E. D. and Graul, T. 1972. Design and Application of Modern High Speed Catamarans. *Marine Tech.*, **9**:345–57.

Insel, M. and Molland, A. F. 1992. An Investigation into the Resistance Components of High Speed Displacement Catamarans. *RINA Trans.*, **134**:1–20.

Michel. H. W. 1961 The Sea-going Catamaran Ship, its Features and its Feasibility. *Internat. Shipbuild. Progress*, **8**(85):390–401.

Moland, A. F., Wellicome, J. F. and Couser, P. R. 1996. Resistance Experiments on a Systematic Series of High Speed Displacement Catamaran Forms: Variation of Length-Displacement Ratio and Breadth-Draught Ratio. *RINA Trans.*, **138**:59–71.

Moland, A. F. and Lee, A. R. 1997. An Investigation into the Effect of Prismatic Coefficient on Catamaran Resistance. *RINA Trans.*, **139**:157–65.

Moland, A. F., Wellicome, J. F., Temarel, P., Cic, J. and Taunton, D. J. 2001. Experimental Investigation of the Seakeeping Characteristics of Fast Displacement Catamarans in Head and Oblique Seas. *RINA Trans.*, **143**:78–97.

Moss, J. L. 1969. Resistance Test Results for 1/12-Scale Models of Three Planing Catamarans. Ship Hydrodynamics Laboratory, University of Michigan.

Müller-Graf, B. 1989. Schnelle Fahrgastkatamarane (High Speed Passenger Catamarans). *Yearbook of STG*, **83**:179–95.

Müller-Graf, B. 1991. The Effect on an Advanced Spray Rail System on Resistance and Development of Spray of Semi-Displacement Round Bilge Hulls. *Proc. 1st FAST Conf.*, Trondheim, pp. 125–41.

Müller-Graf, B. 1993a. Der Einfluß der Spantsymmetrie auf Widerstand, Leistungs-bedarf und Seeverhalten von schnellen Gleitkatamaranen (The Effect of Section Symmetry on Resistance, Powering Performance and Seakeeping Qualities of High Speed Planing Catamarans). *Yearbook of STG*, **87**:206–13.

Müller-Graf, B. 1993b. The Scope of the VWS Hard Chine Hull Catamaran Series '89. *Proc. 2nd FAST Conf.*, Yokohama, pp. 223–37.

Müller-Graf, B. 1993c. Widerstand und Propulsion-Erste Ergebnisse der VWS-Gleitkatamaran-Serie '89 (Resistance and Propulsion – First Results of the VWS Fast Hard Chine Hull Catamaran Series '89). Erweiterter Text der Arbeit für das Statusseminar des BMFT 1993, VWS-Report 1230/93, Berlin Model Basin, pp. 1–54.

Müller-Graf, B. 1994. Die hydrodynamischen Eigenschaften der VWS-Gleitkatamaran-Serie '89 (The Hydrodynamic Characteristics of the VWS Fast Hard Chine Hull Catamaran Series '89). *Yearbook of STG*, **88**:205–18.

Müller-Graf, B. 1995. Alternative Propeller Concepts for High Speed Planing Hull Catamarans. *Proc. 3rd FAST Conf.*, Lübeck-Travemünde, pp. 977–89.

Müller-Graf, B. 1996. Gütegrade der Propulsion von Gleitkatamaranen (Propulsive Coefficients of the VWS Hard Chine Planing Hull Catamaran Series '89). VWS Report No. 1255/96, Part I, II and III, Berlin Model Basin.

Müller-Graf, B. 1997. General Resistance Aspects of High Speed Small Craft, Part I. *25th WEGEMT*, Athens, pp. 1–75.

Müller-Graf, B. 1999a. Leistungbedarf und Propulsionseigenschaften der shnellen Knickspant-Katamarane der VWS Serie '89 (Power Requirement and Propulsive Characteristics of the VWS Hard Chine Planing Hull Catamaran Series '89). *20th Symp. Yachtenwurf und Yachtbau*, Hamburg, pp. 1–117.

Müller-Graf, B. 1999b. Widerstand und hydrodynamische Eigenschaftender schnellen Knickspant-Katamarane der VWS Serie '89 (Resistance and Hydrodynamic Characteristics of the VWS Fast Hard Chine Catamaran Series '89). *20th Symp. Yachtenwurf und Yachtbau*, Hamburg, pp . 1–121.

Müller-Graf, B. 2000. The Components of the Propulsive Efficiency of the VWS Fast Hard Chine Hull Catamaran Series '89 and their Application to the Power Prediction. *Proc. IMAM Conf.*, Ischia, pp. 1–25.

Radojcic, D. 1988. Mathematical Model of Segmential Section Propeller Series for Open-Water and Cavitating Conditions Applicable in CAD. *Proc. SNAME Propellers '88 Symp.*, Virginia Beach, pp. 5.1–5.24.

Radojcic, D. 1991. An Engineering Approach to Predicting the Hydrodynamic Performance of Planing Craft Using Computer Techniques. *RINA Trans.*, **133**:251–67.

Radojcic, D., Matic, D. 1997. Regression Analysis of Surface Piercing Propeller Series. *Proc. 4th HSMV Conf.*, Sorrento, pp. 2.3–2.12.

Radojcic, D., Rodic, T. and Kostic, N. 1997. Resistance and Trim Prediction for the NPL High Speed Round Bilge Displacement Hull Series. *RINA Proc. on Power, Performance and Operability of Small Craft*, Southampton, pp. 10.1–10.14.

Radojcic, D. Princevac, M. and Rodic, T. 1999. Resistance and Trim Predictions for the SKLAD Semidisplacement Hull Series. *Oceanic Engineering Internat.*, **3**(1):34–50.

Radojcic, D. Grigoropoulos, G., Rodic, T., Kuvelic, T. and Damala, D. 2001. The Resistance and Trim of Semi-displacement, Double-Chine, Transom-Stern Hull Series. *Proc. 6th FAST Conf.*, Southampton, **3**:187–95.

Thomas, P. A. 1970. The Aquarius, A Major Development in High Speed Water Transportation. SNAME South East Section.

Turner, H. and Taplin, A. 1968. The Resistance of Large Powered Catamarans. *SNAME Trans.*, **76**:180–213.

Werenskiold, P. 1990. Design Tool for High Speed Slender Catamarans. *Proc. of High Speed Marine Craft Conf.*, Kristiansand, pp. 1–8.

Yermontayev, S., Alframeyev, E. A. Teder, L.A. and Rabinowich, Y. S. 1977. Hydrodynamic Features of High Speed Catamarans. *Hovercraft and Hydrofoil*, **16**(11-12):45–8.

Zips, J. M. 1995. Numerical Resistance Prediction based on the Results of the VWS Hard Chine Catamaran Hull Series '89. *Proc. 3rd FAST Conf.*, Lübeck-Travemünde, pp. 67–74.

APPENDIX 1

Table 3 – Polynomial terms, regression coefficients and important statistics for ε_R

ε_R			$Fn_{\nabla/2}$									
b	c	d	0.50	0.75	1.00	1.25	1.50	2.00	2.50	3.00	3.50	4.00
0	0	0	-0.173909006	-112.2651783	-509.5614157	-31.32927612	-6.483827938	-213.9264914	-5.538630171	580.110804	54.27603261	-184.6978916
0	0	1/3	0.098273967	294.2994508	1408.766278	19.14025823		539.9987966		-1605.025331	-66.19286297	914.8184421
0	0	1/2		-199.8506111	-994.5100187			-370.4512859	-9.917725821	1114.673987		-699.4893401
0	0	1		11.28655	68.12267465		1.787214421	25.31768871	7.541644475	-66.93925993	14.77337705	32.83829292
0	0	2	-0.000929905		-0.650371987	-0.15071261	-0.157478409	-0.375827222	-0.545922051	0.078326823	-0.780955509	1.632325762
0	0	3	4.79565E-05	-0.002683374	0.003227611	0.005329248	0.004460691	0.006446521	0.016109245	0.014394597	0.018708262	-0.067066879
0	1/3	0	1.40197501	-0.111023232	28.89895758			5.0316972		8.206185884		-34.43201745
0	1/3	1	-0.373589592	-0.044838426		-0.424619179		-0.753512558		-1.275464296	0.932429098	3.54204066
0	1/3	2	0.020557836	-0.001122606	0.004875129	0.031895407	0.013447629	0.046551082		0.158227557		-0.050695694
0	1/3	3	-0.000773178	0.000110826	0.000289405	-0.000640324	0.000773728	-0.00041311			0.007031444	0.010607503
0	1/2	0			-29.85438839	0.770268435	0.077603426	-3.532728525	3.855052774		0.1485776	
0	1/2	1		0.111640079		0.236867941		0.480056793	-1.079438402	-0.602500625	-1.053511336	5.919370038
0	1/2	2	0.012565673	-0.004349477	-0.004101338	-0.018451146	-0.011978316	-0.027533194	0.098886531		-0.01126624	-0.814803057
0	1/2	3	-0.000272806		-0.000259073	0.000356916	-0.000684932		-0.003000144	-0.003750377	-0.004510684	0.018031341
0	1	0	-0.052890922	-0.11416155	3.482000005	-0.15451443	-0.03429308		-0.00236895		1.06464733	-1.133737713
0	2	2	-7.32486E-05	1.06422E-05	0.000135917		0.000333708	0.000199097	6.05472E-05	0.001351622	0.00129706	0.002401113
0	3	0				-0.003437854	0.011157241		-0.003847711	0.061737442	0.060719114	-0.063958353
0	3	1/3	5.54611E-06	0.00022107	-0.009114445	0.006701751	-0.030525933	-0.002236196	0.003141962	-0.170204772	-0.18277075	0.019759093
0	3	1/2			0.007117478	-0.003990541	0.021737137	0.003218849		0.11997211	0.128987686	0.027020249
0	3	1	4.01738E-05	-3.6942E-05	-0.000632067	0.000162902	-0.001584395	-0.000631249	-0.000333281	-0.008100977	-0.008262745	-0.007566737
1/3	0	0		96.43339632	169.5730735	32.94677916	-273.8738375	23.91614886	16.37966409		-50.03192156	1065.910968
1/3	0	1/3	0.009026319	-248.0043541	-454.6815211	-19.99056577	782.3842726				64.55774071	-3400.216618
1/3	0	1/2		166.1281198	311.7049875		-557.5559477	-17.87113665		26.14833521		2480.012934
1/3	0	1	0.003117269	-8.698809939	-18.03232553		38.40772215	3.459033128	-4.847018415	-15.05328	-15.21465888	-163.0347301
1/3	0	2	-0.000367979	-0.035862798		0.154586141	-0.337995278		0.469421912	0.941812585	0.836166796	
1/3	0	3		0.003138442	0.004637667	-0.005429348	0.001123062	-0.001945232	-0.014796664	-0.02617229	-0.020484234	0.048761198
1/3	1/3	0		-1.800692237	-1.054333112		-0.953287538	-9.988112947	-1.426699542	-21.43073246		-47.73068432
1/3	1/3	1/2	1.067690131			0.315020592			0.754873832	7.050646806	2.813607718	-155.6303109
1/3	1/3	2	0.002477064	0.001171068		-0.004374674		-0.006515007	-0.010719862	-0.070689132	-0.026902607	0.392691486
1/3	1/3	3	0.000592035	9.70116E-06	1.05017E-05		4.35928E-05	0.000243565	0.002221158	0.003126801	-0.001061452	-0.027985432
1/3	1/2	0	-1.887287619	2.02892835	0.923845326	-0.651101585	0.83544657	6.759523003	-9.537350769	5.054527124	-5.710893352	
1/3	1/2	1/3		-0.29069583			-0.015614588	1.032769296	5.760080214			193.961622
1/3	1/2	2	-0.018807273		-0.000134816	0.001996301			-0.049218579	-0.025723379	0.014243209	0.430347911
1/3	1	3	8.11248E-05	6.929E-06				1.6761E-06	0.000193775	0.000125952	0.000151197	-0.001713867
1/3	2	0			0.007377176					-0.002691251		0.725363274
1/3	2	1/3	0.018872648	-0.007514197	-0.008648184	0.000561973	-0.007775974	-0.054719271		-0.024054204		-3.065263968
1/3	3	0	0.002719157	-2.99538E-05		0.00276436	-0.000406371		-2.37297E-05		0.006042155	0.069087066
1/3	3	1/3	-0.005103748		-0.00106922	-0.003154042	0.00063966					0.002504611
1/3	3	1/2	0.001985174	0.000225926	0.00088977	0.001295074		0.00174897		0.000861132	-0.001671212	0.064193812
1/2	0	0	0.072769398	-5.604150947		-12.91833009	180.1694818	70.96269449	79.04905394	35.01637327	195.0958416	-409.9154412
1/2	0	1/3	-0.064880292	6.381763374	-8.078625842	7.8291102	-510.0190665	-226.4090839	-245.3440866	-102.6309835	-520.0213187	1309.600381
1/2	0	1/2			11.02867858		363.6322784	169.3310362	177.4981092	64.86303216	354.4516232	-955.6305107
1/2	0	1	0.006109663	-1.373949176	-2.662200029		-25.57633917	-13.31164085	-11.52650546		-19.99299914	62.87849545
1/2	0	2		0.075233486	0.124254964	-0.06031789	0.264623868	0.155452352		-0.28140209		
1/2	0	3		-0.001941525	-0.00327813	0.002114272	-0.001965884	-0.001102358	0.003470766	0.009054415	0.004301751	-0.018832291
1/2	1/3	0	-0.157843141	0.801038942	0.109010834	-3.742590843	-0.04034625			20.90150556	-4.464375693	-19.13790349
1/2	1/3	2	-0.014155953								0.003653487	-0.319682075
1/2	1/3	3	0.000215954	7.109E-06		0.000229064	-0.000164645		-0.000727262	-0.000892853	0.000801927	0.016699922
1/2	1/2	0	1.38760275	-9.468603218		3.461746384		1.305224198	-9.201836071	-38.99368765	-14.33114167	28.93511436
1/2	1/2	1/3	-0.857139387	24.22346633	-0.006271063	0.381620313			37.96795411	72.07499564	59.07406792	-62.71812853
1/2	1/2	1/2		-17.27538509				-0.572817096	-29.99605577	-56.82947363	-43.62868441	42.06281945
1/2	1/2	1	0.068063834	1.253394711	-0.009874787	-0.038159823		0.054841699	2.401100421	4.416686893	3.175312549	1.853727599
1/2	1/2	2	0.015791792	-0.016039311			-5.92686E-05		-0.01476285	-0.029411169	-0.037819984	-0.038702724
1/2	1/2	3	-0.0003327	0.000161663		-0.00019544	0.000146368	-3.58478E-05	0.000425268	0.00060616		-0.005256035
1/2	1	0			-0.096847187			-0.534546754		0.705755958		
1/2	1	1/3		0.03130043	0.023652758	-0.352931053	0.017122595	0.189678093		1.579376224		0.431205275
1/2	1	1	-0.01943599	0.002942045	0.005742715	0.025398792		0.012981352	0.001442397	-0.094369396	-0.014264536	-0.662864429
1/2	1	3	-1.71375E-05			1.66244E-05	-1.31558E-05		-7.85099E-05	-7.35919E-05	-2.83782E-05	0.000992367
1/2	2	0	-0.015355228	0.000833844	0.004159775	-0.025219485		0.016518287			-0.072182961	-0.530956629
1/2	2	1/3	0.012297817			0.02209567	-0.000780421	-0.0031847		-0.034490417	0.031491026	0.356916231
1/2	2	1	-0.000717806	-0.000196319	-0.000422623	-0.001488523	-3.05483E-05	-0.000992014		0.001824472		-0.016747648
No. of cases			264	264	264	264	264	264	264	264	264	264
df			42	46	42	43	41	44	40	48	46	55
R^2			0.9974	0.9942	0.9992	0.9999	0.9997	0.9996	0.9994	0.9992	0.9979	0.99692364
F - test			2014	811	6718	39912	18292	12573	9690	5825	2316	1225.50
Standard error			0.00006	0.00016	0.00018	0.0002	0.00025	0.00027	0.00036	0.00045	0.00057	0.00077

Tab. 4 Polynomial terms and reg. coeff. for $1-t_X$

$1-t_X$				
a	d	β_M = 16°	β_M = 27°	β_M = 38°
0	0	582.9743125	3530.92917	-2952.250041
0	1/3	-838.4031467	-555.7488296	2915.266617
0	2/3			-651.8353445
0	1	339.8417169		
0	4/3	-79.55660778		
0	7/3		1.017677851	
0	8/3		-0.401288534	-6.778659381
0	3			0.253753953
1/3	0		-15889.25018	-8691.700501
1/3	1/3		1449.326105	32866.94837
1/3	2/3	198.4283211		-40696.84803
1/3	1			23438.65409
1/3	4/3	-168.066824		-7022.837312
1/3	5/3		-3.878573982	946.5143988
1/3	7/3	2.815640455		
1/3	8/3			30.0641125
1/3	3		0.098489155	
2/3	0		29154.37403	-3226.456924
2/3	1/3			3163.820203
2/3	2/3		70.48878096	
2/3	4/3	-45.53842418		-62.53581857
2/3	5/3	112.8178962		
2/3	8/3	-1.141304574		-75.6709209
2/3	3		-0.058671275	0.6087716
1	0	18.02983154	-27517.47395	
1	1/3		-4183.896989	-971.0872708
1	2	-31.07238746		
1	7/3		0.159722886	
1	8/3			88.74811477
1	3			-0.301893841
4/3	0		14305.11034	508.4011427
4/3	1/3	-81.98165886	5376.565056	
4/3	2/3			62.3800766
4/3	8/3	2.403544674		-56.68667611
5/3	0		-4268.871359	
5/3	1/3		-2473.698695	
5/3	2/3	41.15628117	-29.48358228	
5/3	7/3	6.159156761		
5/3	8/3	-2.963818778		17.06406637
2	0		979.8949915	
2	1/3			-42.77319845
2	2/3		18.58967113	
2	5/3	-4.564213563		
2	3	0.248764782		
7/3	0	10.14775785	-226.8268865	
7/3	1/3	-12.8881988	335.6204244	
7/3	1	2.543686791		
7/3	5/3		-0.104261691	
7/3	8/3		0.002045042	-1.039991459
7/3	3	-0.217205516		
8/3	1/3		-78.13967182	
8/3	1			1.916823684
8/3	8/3	-0.05608642		
8/3	3	0.129735341		
3	0		13.15790177	
3	5/3			-0.131867724
3	7/3	0.040025677		
3	8/3			0.057518745
3	3	-0.024540346		

Tab. 5 Polynomial terms and reg. coeff. for η_H

η_H				
a	d	β_M = 16°	β_M = 27°	β_M = 38°
0	0	-448.919705	-6.868901638	-74.00031245
0	1/2	390.397		
0	1	-85.7596		-35.9982441
0	3/2			-7.590026496
0	3	0.051240292		
0	9/2		-2.54393E-05	0.00040135
1/2	0	930.1355384	137.8197734	104.4439706
1/2	1/2	-874.1077809	-5.412922148	
1/2	1	207.3036743		289.9352487
1/2	5/2		0.000912759	0.722602252
1/2	3	-0.127501358		
1/2	4			-0.008513543
1/2	9/2		4.14494E-06	
1	0	-563.8221973	-438.653638	-39.57092486
1	1/2	609.4217601		-19.22645858
1	1	-169.6183198		-528.8288202
1	2			-1.54945618
1	3	0.107077275		
1	9/2			0.001241681
3/2	0		540.6594967	
3/2	1/2		58.27922647	
3/2	1			308.8733906
3/2	3/2	10.05251429		
3/2	5/2	-0.295290847		
3/2	3		0.017719729	
3/2	9/2			-0.000462956
2	0		-253.0026209	
2	1/2	-32.22046574	-117.4065953	
2	1			325.9841841
2	3/2			2.09991534
2	2			-0.394290073
2	5/2		-0.167056815	
2	3			0.011639937
5/2	0			3.457922799
5/2	1/2		80.28435191	
5/2	1			-694.4983496
5/2	2		0.681567816	
5/2	7/2			0.000446629
3	0	24.67086115		
3	1			535.9963016
3	3/2	-0.138223976	-1.511624376	
3	9/2		-1.88987E-07	
7/2	0	-10.9378	40.33427999	
7/2	1/2		-26.35622515	
7/2	1		1.90388232	-221.3579359
7/2	3/2	0.085793454		
7/2	4	4.09031E-05		
7/2	9/2	-6.49539E-06		
4	0	1.13999888	-23.00596965	
4	1/2		11.0279156	
4	1	0.130195846		48.52956223
4	3/2	-0.044670575		
4	7/2			-5.14165E-05
9/2	0		4.140266787	
9/2	1/2		-1.803444086	-0.034293017
9/2	1			-4.442852827
9/2	3/2		-0.00012659	
9/2	9/2		2.52155E-08	6.35951E-07

Tab. 6 Polynomial terms and reg. coeff. for θ

θ				
a	d	β_M = 16°	β_M = 27°	β_M = 38°
0	0	-634.6364094	18463.00301	1839.125226
0	1/3		-11497.74607	
0	1		-29.06759571	
0	4/3	604.6621485		
0	7/3	-65.01351656	-0.073450332	
0	3			-11.54115526
1/3	0		-50269.1766	
1/3	1/3	1060.793057	42073.7678	
1/3	2/3			-9402.757876
1/3	1			8983.26982
1/3	4/3	-2162.533542		-2788.014903
1/3	5/3		4.383497838	
1/3	2			110.025186
1/3	7/3	259.2957698		
1/3	3			57.26172282
2/3	0	-460.20542		
2/3	1/3		-46581.76531	
2/3	4/3	2487.412038		
2/3	2			-2.172519882
2/3	7/3	-377.0172583		
2/3	3			-121.0950009
1	0		127172.7946	
1	4/3	-1265.835277		
1	2	180.7786529		
1	7/3	162.61378	-0.186971675	
1	3	0.888384857		133.420572
4/3	0		-153939.4243	11241.24289
4/3	1/3		32269.22872	
4/3	2		-0.098061479	
4/3	3			-80.33049354
5/3	0		61414.01976	-13293.77781
5/3	1/3	48.74603199	-17162.13935	
5/3	2	-187.8661802		
5/3	7/3			0.644877162
5/3	3			22.73054976
2	5/3	228.0192776		
2	7/3	7.954483913		
7/3	0			7639.734977
7/3	4/3	-10.98788879		
7/3	7/3			-0.295338037
7/3	8/3		0.027083457	
7/3	3	-1.049603559		-1.493165472
8/3	0		-4192.139521	-4391.407319
8/3	1/3		1460.905499	
8/3	5/3	-58.62118585		
8/3	7/3	3.858210486		
8/3	8/3		-0.01271968	
8/3	3	0.65207657		0.242860882
3	0		1250.279699	778.622157
3	1/3		-447.3178958	
3	5/3	14.9056878		
3	2			0.07440728
3	8/3	-0.774905725		

Tab. 7 Polynomial terms and reg. coeff. for η_D

η_D				
a	d	β_M = 16°	β_M = 27°	β_M = 38°
0	0	-1697.527857	-3012.583635	-12558.53639
0	1/4	-208.6648087		-3054.761894
0	1/3			5731.260446
0	1/2			-2102.151272
0	5/4	3295.227999	-120.5308326	
0	3/2	-4563.078591	172.7186711	
0	7/4	2302.038967	-93.84143003	
0	2	-361.0569613	37.58570491	
1/4	0	4500.543705	39616.96581	133642.4443
1/4	5/4	-4414.227614		
1/4	7/4	-1116.935008		
1/4	2	238.8224427	-219.1974048	
1/3	0		-53801.22937	-169070.9407
1/3	3/4			2037.346532
1/3	5/4	10423.73127		-71.302054
1/3	2		272.7511588	
1/2	0		18485.76499	47840.95943
1/2	1/2	-11771.39585		-8233.130491
1/2	3/4	8039.352139		
1/2	1	-11420.54045		
1/2	7/4		114.5430105	
1/2	2		-109.1135012	0.582095725
3/4	1/3			11729.76897
3/4	1/2	10338.64064		
3/4	3/2		-286.0566599	
3/4	2	-2.457312631	17.12690239	
1	0		-2287.002321	
1	1/4		1409.688496	
1	1/3			3116.363331
1	5/4		351.9875623	
5/4	0	-8532.553146		
5/4	1/4			-21171.56317
5/4	1/2		-1543.092524	
5/4	3/2	78.50071312		
5/4	2	-5.640828598		0.025605665
3/2	0	10811.93813		
3/2	1/4	-4334.196865	1012.501108	17622.34797
3/2	1/2			-177.6292385
3/2	3/4		455.7213029	
3/2	1		-211.195996	
3/2	3/2	-16.75099908		
7/4	0	-3129.261281		-32.75621964
7/4	1/4	1682.420119	-302.914761	-6141.698763
7/4	7/4		-0.048595877	
7/4	2			-0.031617283
2	0	-28.96904765	5.602032506	-11.98810005
2	1/4			852.5390077
2	5/4		2.516913432	
2	3/2			0.200206915
2	7/4	-2.96099444		
2	2	1.275101545		

Tab. 8 Polynomial terms and reg. coeff. for $1\text{-}w_T$

$1 - w_T$				
a	d	β_M = 16°	β_M = 27°	β_M = 38°
0	0	-116.1918809	191.5348352	1351.4812
0	1/2	40.67382787		-1128.195122
0	1		-0.217881315	812.3062999
0	3/2			-238.9348394
0	2	4.174948152		28.17577708
0	3	-0.330798043		
0	7/2		-0.000543264	
0	4	0.004183984	9.72812E-05	-0.019268611
1/2	0		-1023.839208	-3925.540889
1/2	1/2	174.2014292		-593.5982772
1/2	3/2	-84.37140405	0.354994523	
1/2	5/2	4.530073464		
1/2	4	-0.002493759		
1/2	9/2			0.01187141
1	0		2353.822124	10910.51458
1	1/2		5.836882114	823.4872384
1	1	-216.9905239	-2.835718617	
1	3/2	302.3030098		0.01278952
1	2	-55.46325021		
1	5/2	-1.045376396		
1	9/2			-0.021605961
3/2	0		-3043.630328	-15843.93045
3/2	1/2	-117.5244542		-457.9694395
3/2	3/2	-188.0468083		
3/2	2	45.57921322		
3/2	5/2		-0.001519587	
3/2	9/2			0.020584912
2	0	204.3949549	2418.832398	12957.0325
2	1	221.122765	1.197713944	
2	2	-12.06524797		
2	9/2			-0.010841703
5/2	0	-217.6285779	-1224.646193	-5717.623437
5/2	1/2			99.9562774
5/2	1	-113.1188212		
5/2	3/2	27.1242057		
5/2	2		0.001708786	
5/2	9/2			0.002996035
3	0	85.75458413	393.8209279	929.2639667
3	1/2	20.11076638	-2.960285905	-30.20825658
3	1	5.04475576	-0.382117113	
3	3/2	-2.940023171		
3	3	0.002537542		
3	9/2			-0.000339686
7/2	0	-16.27160518	-75.26366791	238.783506
7/2	1/2		2.370759179	
7/2	1	0.595567253	0.09044661	
4	0		6.629323052	-122.882507
4	1/2		-0.487424751	
4	1			-0.001618597
9/2	0			14.59114828
9/2	1/2			0.26419112

Tab. 9 Polynomial terms and reg. coeff. for η_O

η_O				
a	d	β_M = 16°	β_M = 27°	β_M = 38°
0	0	-539.9646094	-323.7314017	-981.9975875
0	1/2	234.2081809	17.24569041	112.8867187
0	1	-53.35882643		11.11428039
0	3/2	5.841191206		
0	2			0.075115522
0	4		1.86686E-05	
1/2	0	1948.958149	1691.837213	4677.669316
1/2	1/2	-488.9153323	-46.54566534	-244.3071136
1/2	1	69.83654546		-103.90154
1/2	3/2	-9.520959406	-0.389623973	
1	0	-3234.571716	-3794.580963	-9801.093132
1	1/2	272.310587	23.50016946	143.3682255
1	1	55.11461414		244.2701654
3/2	0	3310.487284	4787.039638	11657.77711
3/2	1	-120.2009263	23.61695962	-243.2524091
3/2	3/2	5.642199369		
3/2	2			-0.271115211
3/2	7/2		-0.000126516	
2	0	-2201.263462	-3626.708217	-8398.299289
2	1	53.70003012	-46.62886027	109.9143262
2	3/2	-1.596561157		
2	5/2		0.005521356	
2	7/2			-0.00017944
5/2	0	883.1813597	1614.474737	3560.79854
5/2	1/2	-11.39852858		
5/2	1	-7.714356531	40.21291005	-26.84909772
5/2	3/2			2.943272484
5/2	5/2			0.043263618
5/2	9/2	7.23797E-06		
3	0	-188.2890989	-357.1686594	-749.0763394
3	1		-19.33755989	
3	2			-0.380231591
3	7/2	-0.000457294		
7/2	0	15.82467515		
7/2	1/2			1.094808976
7/2	1		5.335715856	
7/2	3		-0.000717967	
7/2	7/2	0.00020496	9.29276E-05	
4	0		16.96658503	31.10439614
4	1/2	0.734772168		0.187102275
4	1		-0.935593781	
4	3/2		0.044879284	
4	2			0.06082328
9/2	0		-2.743963291	-4.399465274
9/2	1/2	-0.135893757	0.237815415	
9/2	2			-0.012714277
9/2	4	-1.69973E-06		
9/2	9/2			-6.91935E-08

Tab. 10 Polynomial terms and reg. coeff. for ε_{BTR}

ε_{BTR}				
a	d	β_M = 16°	β_M = 27°	β_M = 38°
0	0	-75.11557898	165.5334799	-96.61876908
0	1/2	180.6528927	-32.08809452	57.60677895
0	1	-59.3416869		
0	3/2	7.129496756	-0.07020208	
0	2	-0.366894267		
1/2	0		-791.0198737	787.1852118
1/2	1/2	-456.8424596	158.2762657	-408.64497
1/2	1	125.148006		
1/2	3/2	-7.735620595	0.197660404	
1/2	3	0.003509819		
1	0	523.2676054	1509.767793	-2427.530358
1	1/2	342.6528228	-308.5285358	1203.907875
1	1	-75.99088211		
1	3/2		-0.179780824	
1	9/2			1.72793E-07
3/2	0	-873.113987	-1458.647011	3768.579813
3/2	1/2		301.4487727	-1923.468882
3/2	3/2		0.057200221	
2	0	525.4931424	730.9175464	-3136.854141
2	1/2	-59.91777426	-151.539806	1819.309177
2	3/2			0.000186355
2	2	1.721986359		
5/2	0	-122.023611	-158.1428026	1240.467831
5/2	1/2	22.00522137	32.66818281	-1035.771938
5/2	2	0.102483347		
5/2	5/2	-0.390363802		
3	1/2	-2.345849016		337.8549472
3	3/2		-0.000947648	
3	3	0.034894497		
3	7/2	0.001194094		
7/2	0			-196.5926231
7/2	1/2			-51.55778092
7/2	7/2	-0.001909626		
7/2	9/2	-1.88073E-05		
4	0	2.015783256	2.67191852	69.75198786
4	1/2		-0.526815762	
4	1	-0.015124225		
4	9/2	1.07596E-05		
9/2	0	-0.380457604	-0.529539213	-8.03394756
9/2	1/2		0.101831902	0.671969008
9/2	3	4.44381E-05		

Tab. 11 Polynomial terms and reg. coeff. for WSC

WSC		
b	d	coeff.
0	0	-963.4005565
0	1/2	173.5484274
1/4	4	3.39391E-05
1/4	1/4	1870.596868
1/4	1/3	-1419.106142
2/3	4	9.9005E-06
1	1/3	-16.12995062
1	2/3	5.942104476
3	3	-7.49963E-07
4	0	2.58292E-05
4	4	6.71128E-10

Tab. 12 Polynomial terms and reg. coeff. for $L_{WL}/(\nabla/2)^{1/3}$

$L/(\nabla/2)^{1/3}$		
b	d	coeff.
0	0	29.96173317
0	1/4	-22.23455773
0	1	2.07593765
0	2	-0.053750199
0	4	0.00028278
1/4	4	-0.000125747
1	2	0.001814593
2	0	0.000212214
2	3/4	-0.001845546
3	1/4	0.000169785
4	0	-3.32164E-06

Table 13 – Important statistics for $1\text{-}t_X$, η_H, θ, η_D, $1 - w_T$, η_O, ε_{BTR}, WSC and $L_{WL}/(\nabla/2)^{1/3}$

	$1\text{-}t_X$			η_H			Θ			η_D			$1\text{-}w_T$			η_O			ε_{BTR}			WSC	$L/(\nabla/2)^{1/3}$
β_M	16°	27°	38°	16°	27°	38°	16°	27°	38°	16°	27°	38°	16°	27°	38°	16°	27°	38°	16°	27°	38°	-	-
df	26	26	28	23	25	28	23	20	21	26	24	22	28	22	28	27	25	28	29	20	19	10	10
R^2	0.988	0.988	0.9916	0.9944	0.9945	0.9903	0.9889	0.9847	0.982	0.9987	0.9978	0.9936	0.9907	0.9857	0.9886	0.9977	0.999	0.9999	0.9983	0.9988	0.9986	0.9996	0.9999
F - test	628	629	826	1558	1447	718	975	818	657	6007	3730	1429	746	635	605	3152	8360	50128	5618	11678	10794	17751	30780
Standard error	0.00355	0.00235	0.00215	0.00436	0.00317	0.00457	0.08623	0.09223	0.11658	0.0028	0.00305	0.00503	0.00324	0.00356	0.00358	0.00216	0.00124	0.00043	0.00492	0.00399	0.00459	0.01502	0.00517
No. of cases	225	225	225	225	225	225	275	275	275	225	225	225	225	225	225	225	225	225	300	300	300	75	75

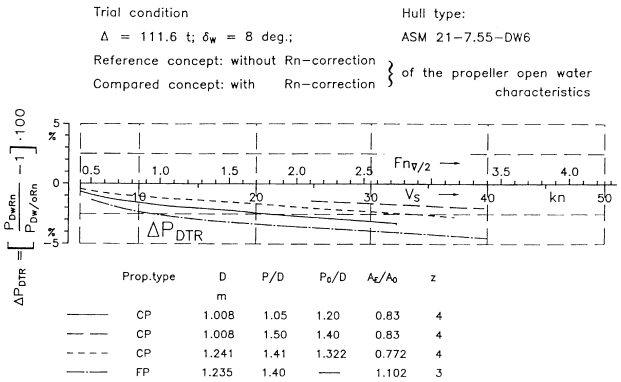

Figure 25 - Relative reduction of propulsive power due to the Rn - correction of the prop. characteristics

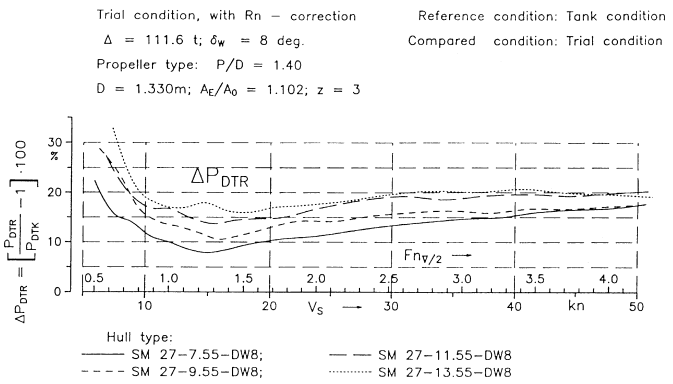

Figure 26 - Relative increase of propulsive power due to the trial condition at $\beta_M = 27^o$

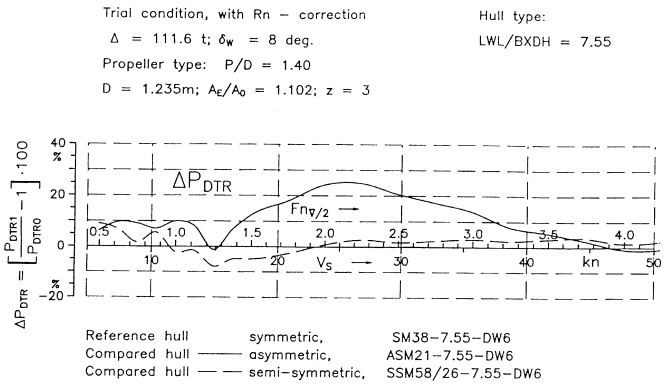

Figure 27 - Relative change of delivered power due to section symmetry at $L_{WL}/B_{XDH} = 7.55$

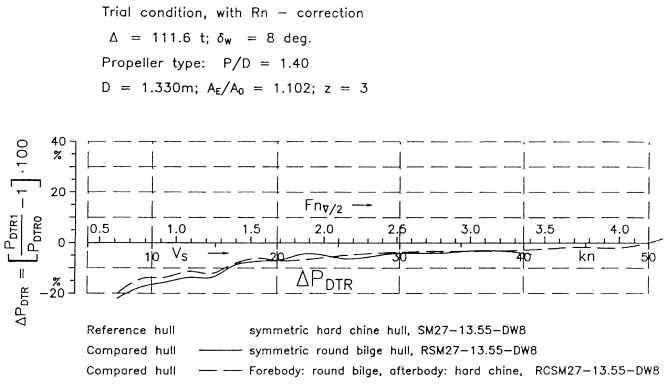

Figure 28 - Relative change of propulsive power due to section form at $L_{WL}/B_{XDH} = 13.55$

APPENDIX 2

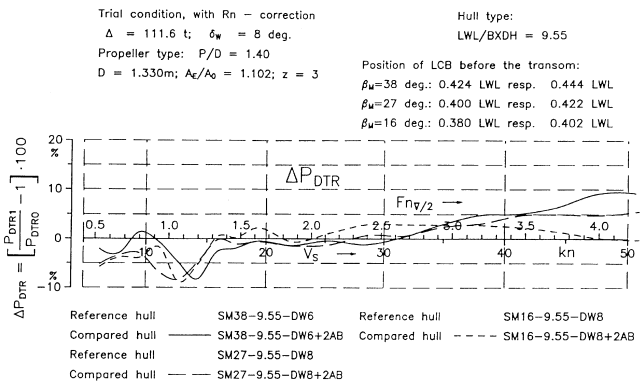

Figure 29 - Relative change of delivered power due to a 2% shift of the longitudinal centre of buoyancy

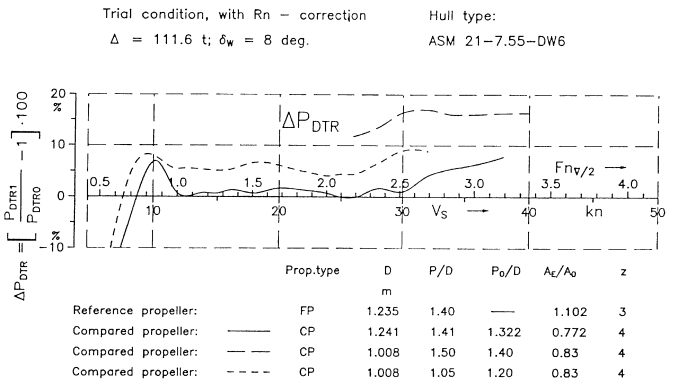

Figure 30 - Relative change of propulsive power due to the effect of the propeller parameter

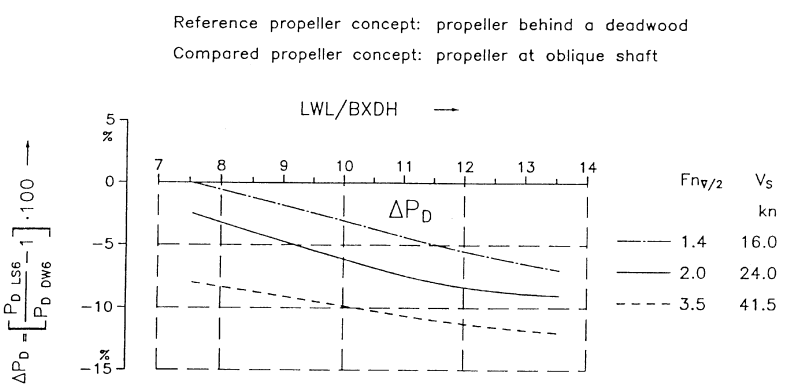

Figure 31 - Relative change of propulsive power due to inclined shafts at $\beta_M = 16^o$

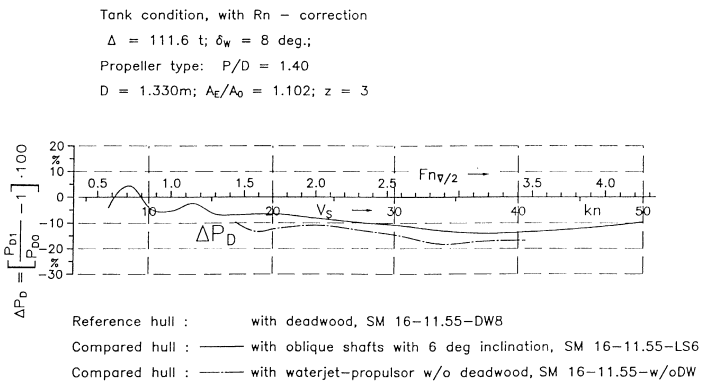

Figure 32 - Relative change of propulsive power due to inclined shafts and waterjets